

## The Fumed Silica Surface: A Study by NMR

Changhua C. Liu<sup>†</sup> and Gary E. Maciel\*

Contribution from the Department of Chemistry, Colorado State University, Fort Collins, Colorado 80523

Received December 7, 1995<sup>⊗</sup>

**Abstract:** High-resolution solid-state NMR techniques were used to investigate the surface structure of Cab-O-Sil fumed silica. <sup>1</sup>H NMR results obtained from CRAMPS, MAS-only and relaxation studies reveal the existence of both hydrogen-bonded silanols and isolated silanols on the Cab-O-Sil surface. A systematic dehydration study of fumed silica was carried out, with results on the quantity of each type of silanol on the surface at various dehydration stages. <sup>29</sup>Si CP-MAS experiments, including CP spin dynamics studies and various other relaxation studies, were employed to probe hydrogen bonding and the local structural environments of various hydroxyl groups of silica surfaces. <sup>29</sup>Si CP-MAS experiments on water-treated and deuterium-exchanged Cab-O-Sil indicate the existence of interparticle silanols and internal silanols in fumed silica. <sup>1</sup>H and <sup>29</sup>Si NMR show that for fumed silica both isolated and hydrogen-bonded silanols are present on the surface of an untreated sample, in contrast to the case of silica gel, where all silanols of an untreated sample are hydrogen bonded.

## Introduction

Cab-O-Sil fumed silica,<sup>1</sup> which is produced at high temperature by the hydrolysis of silicon tetrachloride vapor in a flame of hydrogen and oxygen, is a nonporous, amorphous silica with high purity (>99.8% SiO<sub>2</sub>). It has unique particle characteristics, such as extremely small particle size, very high surface area and chain-forming tendencies. The amorphous nature of Cab-O-Sil is caused by extremely rapid cooling of the silica aggregates, which takes place in a few thousandths of a second. The true density of the aggregate is 2.20 g/cm<sup>3</sup>, but the bulk density of unpressed Cab-O-Sil silica is much lower, approximately 0.032 g/cm<sup>3</sup>.<sup>1</sup>

Because the widespread utility of amorphous silicas, e.g., in sorption, heterogeneous catalysis, and composite materials, is largely a result of their surface properties, studies of the structures, chemistry, and properties of a variety of fumed silica surfaces have been carried out by many researchers for many years.<sup>2–52</sup> Careful analysis by a variety of methods has shown

that the surface reactivity of a silica depends substantially on the quantity and structural environment of its surface hydroxyl groups, which in turn depend on the origin of the silica and its

- \* To whom correspondence should be addressed.  
<sup>†</sup> Current address: Pharm-Eco Laboratories, Inc., 128 Spring Street, Lexington, MA 02173.  
<sup>⊗</sup> Abstract published in *Advance ACS Abstracts*, May 1, 1996.  
 (1) Manufacturer: Cabot Corporation, Boston, MA.  
 (2) Kiss, J. T.; Pálínkó, I.; Molnár, H. *J. Mol. Struct.* **1993**, *293*, 273.  
 (3) Morrow, B. A.; McFarlan, A. J. *J. Phys. Chem.* **1992**, *96*, 1395.  
 (4) McFarlan, A. J.; Morrow, B. A. *J. Phys. Chem.* **1991**, *95*, 5388.  
 (5) Gallas, J. P.; Lavalley, J. C.; Burneau, A.; Barres, O. *Langmuir* **1991**, *7*, 1235.  
 (6) Morrow, B. A.; McFarlan, A. J. *Langmuir* **1991**, *7*, 1695.  
 (7) Burneau, A.; Barres, O.; Gallas, J. P.; Lavalley, J. C. *Langmuir* **1990**, *6*, 1364.  
 (8) Morrow, B. A.; McFarlan, A. J. *J. Non-Cryst. Solids* **1990**, *120*, 61.  
 (9) Chukin, G. D.; Apretova, A. I. *J. Appl. Spectrosc.* **1989**, *50*, 418.  
 (10) Mathias, J.; Wannemacher, G. *J. Colloid Interface Sci.* **1988**, *125*, 61.  
 (11) Lygin, V. I.; Shchepalin, K. L. *Russ. J. Phys. Chem.* **1988**, *62*, 1084.  
 (12) Hoffmann, P.; Knozinger, E. *Surf. Sci.* **1987**, *188*, 181.  
 (13) Gobet, J.; Kováts, E. sz. *Adsorpt. Sci. Technol.* **1984**, *1*, 77.  
 (14) Pavlov, V. V.; Tertykh, V. A. *Teor. Eksp. Khim.* **1975**, *11*, 415.  
 (15) Fripiat, J. J.; Uytterhoeven, J. *J. Phys. Chem.* **1962**, *66*, 800.  
 (16) Davydov, V. Y.; Kiselev, A. V.; Zhuravlev, L. T. *Trans. Faraday Soc.* **1964**, *60*, 2254.  
 (17) Doremus, R. H. *J. Phys. Chem.* **1971**, *75*, 3147.  
 (18) Morrow, B. A.; Cody, I. A. *J. Phys. Chem.* **1973**, *77*, 1465.  
 (19) Morrow, B. A.; Cody, I. A. *J. Phys. Chem.* **1976**, *80*, 1998.  
 (20) Ghiotti, G.; Garrone, E.; Morterra, C.; Boccuzzi, F. *J. Phys. Chem.* **1979**, *83*, 2863.

- (21) Tyler, A. J.; Hambleton, F. H.; Hockey, J. A. *J. Catal.* **1969**, *13*, 35.  
 (22) Hambleton, F. H.; Hockey, J. A.; Tyler, J. A. *Trans. Faraday Soc.* **1966**, *62*, 801.  
 (23) Davydov, V. Y.; Kiselev, A. V. *Russ. J. Phys. Chem.* **1963**, *37*, 1404.  
 (24) Davydov, V. Y.; Zhuravlev, L. T.; Kiselev, A. V. *Russ. J. Phys. Chem.* **1964**, *38*, 1108.  
 (25) Davydov, V. Y.; Kiselev, A. V.; Lokutsievskii, V. A.; Lygin, V. I. *Russian J. Phys. Chem.* **1974**, *48*, 1342.  
 (26) Bermudez, V. M. *J. Phys. Chem.* **1971**, *75*, 3249.  
 (27) McDonald, R. S. *J. Phys. Chem.* **1958**, *62*, 1168.  
 (28) Brei, V. V. *J. Chem. Soc., Faraday Trans.* **1994**, *90*, 2961.  
 (29) Legrand, A. P.; Taibi, H.; Hommel, H.; Tougne, P.; Leonardelli, S. *J. Non-Cryst. Solids* **1993**, *155*, 122.  
 (30) Brei, V. V. *J. Appl. Spectrosc.* **1992**, *56*, 209.  
 (31) Gay, I. D.; McFarlan, A. J.; Morrow, B. A. *J. Phys. Chem.* **1991**, *95*, 1360.  
 (32) Tuel, A.; Hommel, H.; Legrand, A. P.; Kovats, S. Z. *Langmuir* **1990**, *6*, 770.  
 (33) Tuel, A.; Hommel, H.; Legrand, A. P.; Chevallier, Y.; Morawski, J. C. *Colloid Surf.* **1990**, *45*, 413.  
 (34) Morrow, B. A.; Gay, I. D. *J. Phys. Chem.* **1988**, *92*, 5569.  
 (35) Gorlov, Y. I.; Brei, V. V.; Samoson, A. V.; Chuiko, A. A. *Theor. Exp. Chem.* **1986**, *24*, 231.  
 (36) Haan, J. W. D.; Ven Den Bogaert, H. M.; Ponjee, J. J.; Van De Ven, L. J. M. *J. Colloid Interface Sci.* **1986**, *110*, 591.  
 (37) Lippmaa, A. E. T.; Samoson, A. V.; Brei, V. V.; Gorlov, Y. I. *Dokl. Phys. Chem.* **1981**, *259*, 639.  
 (38) Bowsher, L. G.; Hall, P. G. *Sep. Sci. Technol.* **1978**, *13*, 335.  
 (39) Prickett, J. H.; Rogers, L. B. *Anal. Chem.* **1967**, *39*, 1872.  
 (40) Zhuravlev, L. T. *Colloids Surf., A: Physicochemical and Engineering Aspects* **1993**, *74*, 71.  
 (41) Nandi, A. K.; Chowdhuri, A. K.; Ghosh, S.; Thiagarajan, S. *Indian J. Phys.* **1992**, *66A*, 281.  
 (42) Valencia, E.; Maldonado, A. *J. Chem. Soc. Faraday Trans.* **1990**, *86*, 539.  
 (43) Schaefer, D. W.; Hurd, A. *J. Aerosol Sci. Technol.* **1990**, *12*, 876.  
 (44) Chuiko, A. A.; Pilyankevich, E. A.; Gette, A. V. *Dokl. Akad. Nauk SSSR* **1990**, *315*, 152.  
 (45) Zaboriski, M.; Vidal, A.; Ligner, G.; Balard, H.; Papirer, E.; Burneau, A. *Langmuir* **1989**, *5*, 447.  
 (46) Gorlov, Y. I.; Mel' nichenko, G. N.; Nazarancko, V. A. *Teor. Eksp. Khim.* **1984**, *20*, 754.  
 (47) Gorlov, Y. I.; Chuiko, A. A.; Tropinov, A. G.; Nazarenko, V. A. *Teor. Eksp. Khim.* **1980**, *16*, 405.  
 (48) Gorlov, Y. I.; Konoplya, M. M.; Chuiko, A. A. *Teor. Eksp. Khim.* **1980**, *16*, 333.  
 (49) Gorlov, Y. I.; Golovaty, V. G.; Konoplya, M. M.; Chuiko, A. A. *Teor. Eksp. Khim.* **1980**, *16*, 202.

storage and treatment conditions.<sup>53</sup> The most widely employed methods of investigation have been the following: IR,<sup>2-27,30,31,36</sup> sometimes with a variety of chemical probes,<sup>6,8,16,22,24</sup> NMR,<sup>28-39</sup> and adsorption techniques.<sup>12,19,20,25,26,31,38,39,42,51</sup>

In spite of the extensive experimental data reported on fumed silica surfaces, a compelling, comprehensive consensus has not yet been reached on important surface chemical details. It has been reported that silanol groups on the fumed silica surface are predominantly isolated from each other, i.e., not hydrogen bonded.<sup>27</sup> These isolated silanols were viewed as randomly distributed by Burneau and co-workers<sup>7</sup> and as uniformly distributed by Pavlov and Tertykh.<sup>14</sup> Morrow and McFerhan<sup>3</sup> recently identified two types of isolated silanol sites on an Aerosil fumed silica surface following vacuum activation at about 450 °C. One of these two types of OH groups is reported to be truly isolated, whereas the other type was described as a weakly interacting "vicinal" type. At about the same time, a structural model of fumed silica was postulated on the basis of X-ray data.<sup>41</sup> According to that model, hydrogen bonding occurs among the entire set, or a large fraction, of the silanols of the fumed silica surface. The Aerosil fumed silica surface is pictured by Barby<sup>54</sup> as having about equal numbers of "isolated" silanols and of "hydrogen-bonded" pairs of silanols. Questions related to the mechanism of dehydration and rehydration of the fumed silica surface also have not been answered to a substantial level of agreement among researchers.<sup>47,48</sup>

One of the most informative methods of studying silica and aluminosilicate structures has been high-resolution solid-state <sup>29</sup>Si NMR spectroscopy, but solid-state NMR techniques have been applied much less to fumed silica systems than to silica gels or precipitated silica systems. The use of <sup>29</sup>Si NMR, especially with cross polarization (CP)<sup>55</sup> and magic-angle spinning (MAS),<sup>56</sup> for the study of silica surfaces was demonstrated on silica gel by Maciel and Sindorf,<sup>57-63</sup> who made use of separate signals for single silanols and geminal silanols. CP-MAS <sup>29</sup>Si NMR spectra of Aerosil fumed silica have also been obtained and interpreted in a similar way.<sup>37</sup> Details of CP dynamics and relaxation properties in <sup>29</sup>Si CP-MAS studies, as well as high-resolution <sup>1</sup>H NMR studies, have provided important details on the surface structures of silica gel.<sup>58-70</sup> However, a comprehensive <sup>29</sup>Si NMR study, in which CP dynamics and/or various relaxation issues are used to elucidate

surface details, has not been published on fumed silica. There have been only two published reports on fumed silica that have involved solid-state <sup>1</sup>H NMR techniques,<sup>35,37</sup> both of which described studies of the dehydration and rehydration of Aerosil silica. The results of these two studies are not in agreement with each other, and the assignments of various peaks in the <sup>1</sup>H NMR spectra have remained unclear.

The syntheses of sol-gel silica (i.e., silica gel) and fumed silica (e.g., Cab-O-Sil) are totally different, and these two types of materials are used in different application areas. It is scientifically interesting and technologically important to compare the surface structures and properties of silica gels and fumed silica systems. On the basis of the extensive and successful solid-state NMR work carried out on silica gels, it would seem that many promising NMR techniques that could be used had not yet been utilized, prior to the present study, to investigate the surface structure of fumed silica. Hence, in the study reported here we have investigated the surface of Cab-O-Sil fumed silicas by a variety of solid-state NMR techniques; and we compare some of the results with those previously reported,<sup>58-70</sup> or determined in this study, on silica gels.

## Experimental Section

**NMR Experiments.** Proton spectra obtained by the CRAMPS technique<sup>64,71</sup> and by single-pulse (MAS-only) experiments were performed at 360 MHz on a severely modified Nicolet NT-360 spectrometer. In the CRAMPS experiments, the BR-24 pulse sequence was used, with a 90° pulse length of 1.1–1.2 μs and a pulse spacing of 3.0 μs; magic-angle spinning employed a spinner based on the design of Gay<sup>72</sup> and operated at speeds of 1.5–2.0 kHz. Data sizes were 256 points; recycle delays were 3 s for almost all the samples.

In each proton CRAMPS experiment, approximately 20–30 mg of the Cab-O-Sil sample was loaded in a 5-mm thin-wall NMR tube with a sample depth of 8–10 mm. This sample size was chosen to yield the best signal-to-noise ratio without suffering a loss of spectral resolution. The sample tube was sealed under vacuum, if external moisture was to be excluded.

The MAS spinning system used in the MAS-only experiments of this study was based on the design of a high-speed/variable-temperature MAS system, using a 4-mm pencil-type zirconia rotor that was developed by Chemagnetics, with air as both the drive and bearing gases. Approximately 20–30 mg of Cab-O-Sil silica was loaded into the rotor, with a tightly fit rotor cap made of Kel-F to exclude outside moisture and avoid spinning off physisorbed water during MAS (*vide infra*). The effectiveness of these rotor caps was judged on the basis that the physisorbed water peak intensity in the <sup>1</sup>H spectrum of an untreated Cab-O-Sil sample was found to change little, and no water peak was introduced into the <sup>1</sup>H spectra of dehydrated samples, after overnight spinning with the cap on. Proton chemical shifts were determined by referencing, via sample substitution, to the <sup>1</sup>H peak of tetrakis(trimethylsilyl)methane (TTMSM) and are reported here relative to tetramethylsilane (TMS) at 0.0 ppm.

<sup>29</sup>Si NMR spectra were obtained on a heavily modified Nicolet NT-200 spectrometer (with a <sup>29</sup>Si Larmor frequency of 39.75 MHz), in most cases with high-power proton decoupling and <sup>1</sup>H–<sup>29</sup>Si cross polarization. The MAS speed was kept constant at 1.6 kHz, unless otherwise indicated in the *Results and Discussion* section. Samples studied by <sup>29</sup>Si NMR were loaded into 2.5 cm<sup>3</sup> MAS rotors of the Pencil type (provided by Chemagnetics), employing Zirconia sleeves and

(50) Gorlov, Y. I.; Konoplya, M. M.; Furman, V. I.; Chuiko, A. A. *Teor. Eksp. Khim.* **1979**, *15*, 446.

(51) Bhamhani, M. R.; Cutting, P. A.; Sing, K. S. W.; Turk, D. H. *J. Colloid Interface Sci.* **1972**, *38*, 109.

(52) Peri, J. B. *J. Phys. Chem.* **1966**, *70*, 2937.

(53) Legrand, A. P.; Hommel, H.; Tuel, A.; Vidal, A.; Balard, H.; Papirer, E.; Levitz, P.; Czernichowski, M.; Erre, R.; Van Damme, H.; Gallas, J. P.; Hemidy, J. F.; Lavalley, J. C.; Barres, O.; Burneau, A.; Grillet, Y. *Adv. Colloid Interface Sci.* **1990**, *33*, 91.

(54) Parfitt, G. D.; Sing, K. S. W. *Characterization of Powder Surfaces*; Academic Press: New York, 1976; p 403.

(55) Pines, A.; Gibby, W. E.; Waugh, J. S. *J. Chem. Phys.* **1973**, *59*, 509.

(56) Andrew, E. R. *Prog. NMR Spectrosc.* **1971**, *8*, 1.

(57) Maciel, G. E.; Sindorf, D. W. *J. Am. Chem. Soc.* **1980**, *102*, 7606.

(58) Sindorf, D. W.; Maciel, G. E. *J. Am. Chem. Soc.* **1983**, *105*, 1487.

(59) Maciel, G. E.; Sindorf, D. W.; Bartuska, V. J. *J. Chromatogr.* **1981**, *205*, 438.

(60) Sindorf, D. W.; Maciel, G. E. *J. Am. Chem. Soc.* **1981**, *103*, 4263.

(61) Sindorf, D. W.; Maciel, G. E. *J. Phys. Chem.* **1982**, *86*, 5208.

(62) Sindorf, D. W.; Maciel, G. E. *J. Am. Chem. Soc.* **1983**, *105*, 3767.

(63) Sindorf, D. W.; Maciel, G. E. *J. Phys. Chem.* **1983**, *87*, 5516.

(64) Maciel, G. E.; Bronnimann, C. E.; Hawkins, B. W. The Waugh Symposium. *Adv. Magn. Reson.* W. S. Warren, ed., **1990**, *14*, 125.

(65) Maciel, G. E.; Bronnimann, C. E.; Zeigler, R. C.; Chuang, I.-S.; Kinney, D. R.; Keiter, E. A. *The Colloid Chemistry of Silica*; Bergna, H. E., Ed.; Adv. Chem. Ser. No. 234; American Chemical Society: Washington, DC, 1994; p 269.

(66) Chuang, I.-S.; Kinney, D. R.; Bronnimann, C. E.; Zeigler, R. C.; Maciel, G. E. *J. Phys. Chem.* **1992**, *96*, 4027.

(67) Chuang, I.-S.; Kinney, D. R.; Maciel, G. E. *J. Am. Chem. Soc.* **1993**, *115*, 8695.

(68) Bronnimann, C. E.; Chuang, I.-S.; Hawkins, B. L.; Maciel, G. E. *J. Am. Chem. Soc.* **1987**, *109*, 1562.

(69) Bronnimann, C. E.; Zeigler, R. C.; Maciel, G. E. *J. Am. Chem. Soc.* **1988**, *110*, 2023.

(70) Kinney, D. R.; Chuang, I.-S.; Maciel, G. E. *J. Am. Chem. Soc.* **1993**, *115*, 6786.

(71) Gerstein, B. C.; Pembleton, R. G.; Wilson, R. C.; Ryan, L. M. *J. Chem. Phys.* **1977**, *66*, 361.

(72) Gay, J. D. *J. Magn. Reson.* **1984**, *58*, 413.

tightly fitting Kel-F drive tips. TTSM was used as an external chemical shift reference (0.024 ppm relative to liquid TMS).

All peak intensities that are stated numerically or utilized to determine a relaxation parameter were obtained from computer-deconvoluted spectra. Most of these deconvolution/simulation spectra are not shown in this paper, but are available elsewhere.<sup>73</sup>

**Samples and Sample Pretreatments.** Three grades of Cab-O-Sil silicas, HS-5, M-5, and L-90, with surface areas of 325, 200, and 100 m<sup>2</sup>/g, respectively, were used. The samples referred to as being "untreated" Cab-O-Sil were simply used as received from the supplier (Cabot Corp.). The silica gel was Fisher S-679 from Fisher Scientific (surface area: 456 m<sup>2</sup>/g).

Humidified samples were prepared by placing untreated silica in a closed container containing an open vessel charged with a saturated solution of NaOH in water at 25 °C to control the humidity in a reproducible manner. The water-treated samples were prepared by slurrying the Cab-O-Sil with water first and then drying in air overnight at room temperature.

To dehydrate a Cab-O-Sil silica, the sample was evacuated in a quartz tube in a tube furnace at  $3 \times 10^{-3}$  Torr at various specified temperatures for various specified lengths of time, usually 6 h. All sample transfers were executed in a glovebox to exclude atmospheric moisture. Samples treated by this process are referred to here by a notation such as HS-5(25 °C), etc., indicating evacuation of HS-5 at 25 °C.

Each deuterium exchange was carried out at room temperature on a 2.0-g sample of the silica powder in a D<sub>2</sub>O-rinsed flask equipped with a D<sub>2</sub>O-rinsed addition funnel filled with D<sub>2</sub>O. After 5 mL of the D<sub>2</sub>O was added to the silica, stirring was continued for about 4 h before the liquid was gradually evaporated under a  $10^{-3}$ -Torr vacuum at 25 °C. Once the D<sub>2</sub>O-exchanged silica was sufficiently dry to flow freely as a powder, a second aliquot of D<sub>2</sub>O was added into the flask. This procedure was repeated three times (four exchanges) without ever opening the flask to air. After the final exchange, the sample was dried at  $10^{-3}$  Torr and 25 °C with stirring of the powder for 12 h.

## Results and Discussion

**<sup>1</sup>H NMR Spectra.** High-resolution <sup>1</sup>H NMR spectroscopy, especially with the CRAMPS technique,<sup>64,71</sup> has proved to be very useful in studying the surfaces of silica and a variety of other solids. With CRAMPS, the potentially severe line-broadening effect associated with <sup>1</sup>H–<sup>1</sup>H dipolar interactions is eliminated via a multiple-pulse sequence and the chemical shift anisotropy is averaged by MAS. MAS-only (single pulse, with MAS detection) averaging of strong, homogeneous dipolar interactions, e.g., among <sup>1</sup>H spin sets in typical organic solids or among <sup>19</sup>F spin sets among fluorocarbon solids, usually requires MAS with speeds comparable to the magnitude of the dipolar interaction, often a difficult requirement to satisfy experimentally. Nevertheless, as MAS technology has improved, some laboratories have relied upon only MAS to average both the inhomogeneous chemical shift effect and the potentially homogeneous line-broadening effect of <sup>1</sup>H–<sup>1</sup>H dipole–dipole interactions. Both CRAMPS and MAS-only <sup>1</sup>H NMR approaches were used in this study. In order to compare these two line-narrowing techniques quantitatively, spin counting experiments employing a <sup>1</sup>H NMR intensity standard were carried out. Details of this spin-counting study are reported elsewhere.<sup>74</sup>

Figure 1 shows the <sup>1</sup>H CRAMPS spectrum of an untreated HS-5 Cab-O-Sil sample and its computer deconvolution/simulation. Figure 2 shows the <sup>1</sup>H MAS-only spectra of the same kind of sample, with a silicone rubber intensity reference added, obtained as a function of spinning speed, ranging from 2 to 12 kHz. The CRAMPS spectrum of the untreated Cab-O-Sil silica shows three major peaks, as seen from the

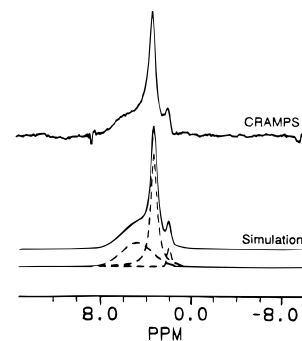


**Figure 1.** <sup>1</sup>H CRAMPS spectrum (top) and its computer simulation/deconvolution (bottom) of an untreated Cab-O-Sil.

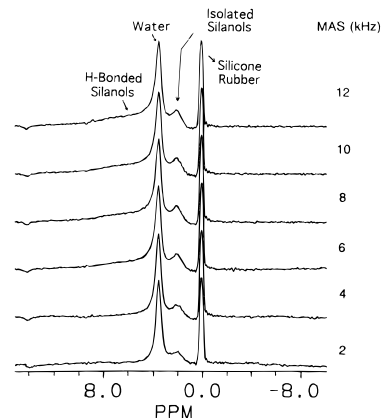


**Figure 2.** <sup>1</sup>H MAS-only spectra of an untreated Cab-O-Sil, with the silicone rubber intensity standard, as a function of MAS spinning speed as indicated.

deconvoluted spectral simulation. The peak at 3.5 ppm is due mainly to water molecules that are physically adsorbed on the silica surface, an assignment that can be derived directly from dehydration studies shown later in this paper, or by analogy to analogous results reported previously on silica gel.<sup>69</sup> The line width of this intense peak is only about 1 ppm, and no MAS sidebands are detected for this peak in the MAS-only spectrum (Figure 2) obtained with about the same MAS speed (2 kHz) as used in obtaining the CRAMPS spectrum (Figure 1). This implies that the water molecules physisorbed on the silica surface have liquid-like behavior, i.e., are rather mobile at the measurement temperature (25 °C). Rapid, random motion essentially averages the <sup>1</sup>H–<sup>1</sup>H dipolar interaction, which otherwise would be tens of kHz in a rigid system and would lead to intense MAS sidebands in the MAS-only spectra. As seen in Figure 2, the mobility of the water molecules in physisorbed water is fast enough to average the <sup>1</sup>H–<sup>1</sup>H dipolar interaction sufficiently so that the line width of this peak is not affected by the MAS spinning speed.

The broad band from about 1 to about 8 ppm in the CRAMPS spectrum is assigned on the basis of earlier silica gel studies<sup>69</sup> to silanol protons in a variety of hydrogen-bonding environments. Hydrogen bonding is commonly identified with proton shifts to lower shielding, and a distribution of types and strengths of hydrogen bonding should yield a distribution of isotropic chemical shifts, i.e., an inhomogeneously broadened peak. In consideration of the strong similarity of the chemical and physical environments of hydrogen-bonded silanol protons and any associated hydrogen-bonded protons of water, it would not be surprising to find that this broad peak overlaps significantly with resonance intensity arising from the protons of water molecules that are strongly hydrogen bonded. With multiple-pulse line-narrowing, the hydrogen-bonded protons are detected,

(73) Liu, C. C. Solid-State <sup>1</sup>H and <sup>29</sup>Si NMR Studies on Cab-O-Sil Silicas Ph.D. Dissertation, Colorado State University, 1995.

(74) Liu, C. C.; Maciel, G. E. *Anal. Chem.* **1996**, *68*, 1401–1407.

**Table 1.** Peak Area and Line Width of Each Deconvoluted Peak in the  $^1\text{H}$  MAS-Only NMR Spectra of Untreated HS-5 Cab-O-Sil as a Function of Spinning Speeds

spinning speed (kHz)	peak area (arbitrary units) <sup>a</sup>			line width (ppm) <sup>b</sup>		
	2.0 ppm <sup>c</sup>	3.5 ppm <sup>d</sup>	5 ppm <sup>e</sup>	2.0 ppm	3.5 ppm	5 ppm
2.0	7.8	51	0	1	0.5	
4.0	11	53	9.2	1	0.6	5.8
6.0	11	54	27	0.9	0.6	5.7
8.0	11	55	29	0.9	0.6	5.5
10	9.0	54	36	0.8	0.6	5.3
12	9.1	55	34	0.8	0.6	5.0

<sup>a</sup> Estimated error:  $\pm 5\%$ . <sup>b</sup> Estimated error:  $\pm 0.1$  ppm. <sup>c</sup> Isolated silanol peak. <sup>d</sup> Physisorbed water peak. <sup>e</sup> Hydrogen-bonded silanol peak.

but their resonance pattern is still rather featureless because of chemical shift dispersion. This broad peak is absent in the low-speed MAS-only  $^1\text{H}$  spectrum (bottom spectrum in Figure 2), a behavior consistent with the interpretation that this peak is due to silanol protons involved in strong dipolar interactions associated with hydrogen bonding, interactions that are too intense to be averaged by low-speed MAS.

From other experiments (e.g., dehydration and dipolar dephasing, *vide infra*, and previously reported studies on silica gel<sup>69</sup>) we know that the resonance at 2.0 ppm is due to protons of *isolated* (i.e., non-hydrogen-bonded) silanols on the silica surface. Observing the bottom spectrum of Figure 2, which was obtained from a MAS-only experiment with a 2.0 kHz spinning speed, two resolved peaks are displayed, the physisorbed water and isolated silanol peaks. The 2.0-kHz MAS speed employed in obtaining this spectrum is sufficient to average both the inhomogeneous CSA effect and the weak  $^1\text{H}$ – $^1\text{H}$  dipole–dipole interactions of protons of isolated silanols, producing a narrow line. The fact that the  $^1\text{H}$ – $^1\text{H}$  dipolar interactions of the isolated silanols are weak enough to be averaged by low-speed MAS reflects some combination of large  $^1\text{H}$ – $^1\text{H}$  internuclear distances and (perhaps) partial averaging of the dipolar interaction by chemical exchange and by rapid rotation of the hydroxyl group around the Si–OH axis<sup>52</sup> (*vide infra*). The spectrum obtained with 4.0-kHz MAS is not substantially different from the 2.0-kHz spectrum. At a 6.0 kHz spinning rate, a broad bump appears in the spectrum centered around 5 ppm (actually the broad bump appears in the 4.0-kHz spectrum as well, but with a smaller intensity, as shown from deconvolutions (not given here));<sup>73</sup> this broad bump is due to hydrogen-bonded silanols, according to the assignment from CRAMPS spectra. This observation is understandable, if the  $^1\text{H}$ – $^1\text{H}$  dipolar interactions experienced by the hydrogen-bonded silanols are so strong (and homogeneous) that this peak can be detected only when the MAS spinning speed is up to a certain value (say, 5–6 kHz). Increasing further the MAS speed does not markedly alter the MAS-only spectra, which are quite similar, in terms of numbers of peaks and relative peak positions, to the corresponding CRAMPS spectrum. Apparently the CRAMPS and high-speed MAS-only  $^1\text{H}$  spectra differ from each other mainly in relatively small variations in the widths and/or relative intensities of the hydrogen-bonded SiOH, isolated SiOH, and physisorbed water bands.

Table 1 summarizes the peak area and line width of each peak in the MAS-only  $^1\text{H}$  spectra shown in Figure 2, as derived from computer deconvolution/simulations (not shown here).<sup>73</sup> The line width of the isolated silanol peak (at 2.0 ppm) is seen to narrow slightly with an increase in the spinning speed, but this peak is reasonably sharp even at 2 kHz. The intensities of the isolated silanol peaks at different spinning rates are similar, but the central peak intensity is smaller at 2 kHz due to the distribution of intensity to weak (unobserved) spinning side-

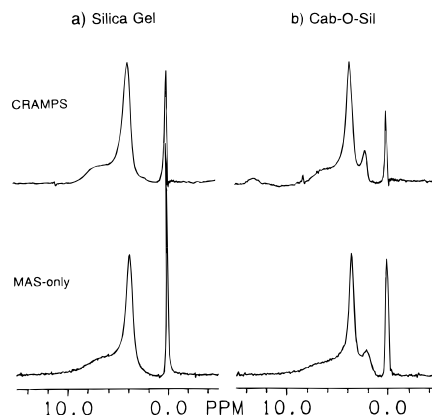


**Figure 3.**  $^1\text{H}$  spectra obtained by CRAMPS (top) and MAS-only with 12-kHz sample rotation (bottom) of untreated (a) silica gel and (b) HS-5 Cab-O-Sil, mixed with silicone rubber (53.1 mg of silica gel was mixed with 1.1 mg of silicone rubber; 29.6 mg of Cab-O-Sil was mixed with 0.30 mg of silicone rubber).

bands. The line width for the hydrogen-bonded silanols is also roughly similar over a range of spinning speeds from 6 to 12 kHz. Clearly, spinning in the 6–12-kHz region is capable of partial averaging of the  $^1\text{H}$ – $^1\text{H}$  dipolar interaction in the hydrogen-bonded silanols. However, one can see that the line width of the band due to hydrogen-bonded silanols is smaller at higher MAS speeds than at lower speeds, and that the observed peak intensity is much higher at 6–12 kHz than at 2–4 kHz, and is substantially smaller at any MAS speed employed than it is in the CRAMPS spectrum of Figure 1. The residual line widths of the hydrogen-bonded silanols in the CRAMPS spectra are determined to a large extent by the distribution of isotropic chemical shift due to the existence of a large variety of hydrogen-bonding structures. In contrast,  $^1\text{H}$ – $^1\text{H}$  dipolar interactions make large contributions to some of the line widths in the MAS-only spectra shown.

Silica gel, silica that has been prepared by condensation of silicic acid from solution, has also been examined for comparison in this study. The  $^1\text{H}$  CRAMPS and 12-kHz MAS-only spectra of an untreated silica gel are shown in Figure 3a. One may notice that the isolated silanol peak at about 2 ppm in untreated Cab-O-Sil silica (Figure 3b) is missing in the  $^1\text{H}$  CRAMPS spectrum of the untreated silica gel sample. In the  $^1\text{H}$  CRAMPS spectrum (not shown here) of another, drier silica gel sample that had been stored in a desiccator for 6 days (6% weight loss), it is obvious that a small resonance at 2 ppm is present in the spectrum. This fact indicates that all of the surface silanol groups in the untreated silica gel system are hydrogen bonded; the occurrence of isolated silanols in the (partially) dried silica gel results from the removal of water molecules in the desiccator, so that at least some of the silanols that were hydrogen bonded only to water in the untreated sample become non-hydrogen bonded in the sample after storage in a desiccator.

The peak at 0 ppm in the spectra shown in Figures 2 and 3 belongs to the internal intensity reference, silicone rubber.<sup>74</sup> Quantitative spin counting results for each spectrum in Figure 3 were obtained in the following two ways: (1) total spectral integration and (2) integration of individual peaks obtained by spectral deconvolution/simulation via computer. After accommodating the relaxation properties of all sample components, and after correction for the weights of silica and silicone rubber used in the two types of experiments and samples, one finds that the MAS-only technique with 12 kHz spinning rate detects essentially the same amount of protons in both Cab-O-Sil silica and silica gel as does the CRAMPS experiment.<sup>73,74</sup> The values obtained in this study<sup>74</sup> for untreated HS-5 and silica gel, 2.8

**Table 2.** Total Integral and Population of Each Proton Species in  $^1\text{H}$  CRAMPS Spectra of Unsealed, Untreated Cab-O-Sil as a Function of Spinning Time

spinning time (h)	total integral <sup>a</sup>	percentage <sup>b</sup>			individual integral <sup>c</sup>		
		5 ppm <sup>d</sup>	3.5 ppm <sup>e</sup>	2.0 ppm <sup>f</sup>	5 ppm	3.5 ppm	2.0 ppm
0	100	30	64	6.0	30	64	6.0
2.0	88	32	60	8.0	28	53	7.0
4.0	72	35	53	12	25	38	9.0
6.0	65	32	52	15	21	34	10
12	58	33	50	17	19	29	10

<sup>a</sup> Obtained by calibration of the intensity standard, estimated error:  $\pm 3\%$ . <sup>b</sup> Estimated error:  $\pm 5\%$ . <sup>c</sup> Integral for each peak, obtained by total integral  $\times$  percentage of each peak. <sup>d</sup> Because of the large line width and asymmetric line shape of the hydrogen-bonded silanol peak, its chemical shift value is only an estimate. <sup>e</sup> Physisorbed water. <sup>f</sup> Isolated silanols.

$\pm 0.3$  and  $6.3 \pm 0.3$  OH/(nm)<sup>2</sup>, are consistent with values obtained by other methods,<sup>75–77</sup> although smaller than some reported values on related materials as studied by NMR techniques.<sup>78</sup> Calibration of the intensity reference and its utility in quantitating  $^1\text{H}$  CRAMPS and MAS-only experiments are described in detail elsewhere.<sup>73,74</sup>

**Dehydration Studies of Cab-O-Sil.** One of the interesting behaviors we observed for Cab-O-Sil silica in this study is that the  $^1\text{H}$  CRAMPS spectrum is changed dramatically when a sample is allowed to spin in a capped, but unsealed MAS rotor for several hours, e.g., overnight. Comparison of  $^1\text{H}$  CRAMPS spectra of an *unsealed* sample of an untreated HS-5 Cab-O-Sil obtained at the beginning and end of a 6-h MAS period (Figure 1a in the Supporting Information) reveals that the physisorbed water peak at 3.5 ppm is decreased in the spectrum obtained after 6 h of spinning relative to the one obtained at the beginning of the experiment, indicating that a substantial change of the sample has occurred during sample spinning. However, when the HS-5 sample is sealed in a glass ampule (by torch), the behavior is different (Figure 1b in the supporting information); in this case the intensity of the water peak is constant with sample spinning time. It seems that the physisorbed water is depleted gradually by spinning an unsealed Cab-O-Sil sample, and sealing prevents the elimination of water from the sample.

To monitor more quantitatively the spinning-induced change of the fumed silica surface,  $^1\text{H}$  CRAMPS spectra were taken periodically when an unsealed Cab-O-Sil sample (mixed with a silicone-rubber intensity standard, yielding a peak at 0 ppm) undergoes MAS over a 12-h period; the resulting spectra are shown in Figure 4.

It appears in Figure 4 that the physisorbed water peak is attenuated as the unsealed sample spins; this is understandable, if the water molecules are only weakly bound to the silica surface, vaporize, and then escape the unsealed rotor. However, besides the attenuation of the water peak, the intensities of both types of silanols are also affected by the MAS duration, as shown quantitatively in the spin counting results given in Table 2. The individual site populations summarized in Table 2 were obtained by computer deconvolutions<sup>73</sup> of the  $^1\text{H}$  CRAMPS spectra and were normalized with respect to the intensity standard. When adsorbed water is removed from the surface, some of the hydrogen bonded silanols, which were originally hydrogen-bonded to water molecules in the untreated sample, become isolated. This results in a gradual intensity increase of the isolated-silanol peak and a decrease in the hydrogen-bonded-silanol peak as the MAS time is increased from 0 to 12 h, as reflected in the results seen in Figure 4 and summarized in Table 2.

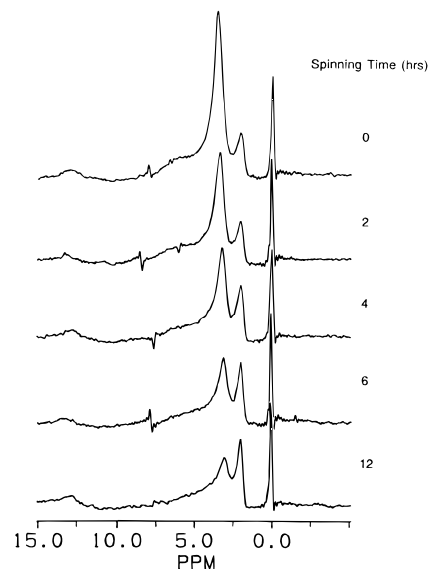


**Figure 4.** A series of  $^1\text{H}$  CRAMPS spectra of an unsealed HS-5 Cab-O-Sil sample, with the intensity reference (25.6 mg, 0.20 mg), as a function of duration of magic-angle spinning.

Thermal dehydration experiments at various temperatures (0–650 °C) and at  $3 \times 10^{-3}$  Torr were carried out on HS-5 Cab-O-Sil silica. Since Cab-O-Sil silica is very sensitive to the humidity to which it is exposed (e.g., in a sample “as received”), an intentionally humidified sample was prepared, as described in the Experimental Section, as a reproducible starting material for the dehydration experiments. Figure 5 shows the CRAMPS spectra of HS-5 Cab-O-Sil that was dehydrated at  $3 \times 10^{-3}$  Torr at various temperatures. The corresponding  $^1\text{H}$  MAS-only spectra, obtained with a 12-kHz MAS spinning speed, are shown in Figure 6; very similar results, except with larger spinning sidebands, were obtained with a MAS speed of 2 kHz (Figure II in the supporting information). All the samples studied in these NMR experiments were mixed with the silicone-rubber intensity standard, which gives rise to the 0-ppm peak seen in all of the spectra.<sup>73,74</sup> Due to the different amount of silicone rubber used in each sample, the height of this peak varies from spectrum to spectrum. Taking spinning sideband intensities into account, one can note, especially for the samples evacuated at temperatures below 350 °C, that the intensity of the hydrogen-bonded silanol band is much weaker in the 2-kHz MAS-only spectra than in the 12 kHz MAS-only spectra of Figure 6, which in turn are weaker than in the CRAMPS spectra of Figure 5.

Comparing the  $^1\text{H}$  CRAMPS spectra of Figure 5 with the spectra obtained as a function of spinning time (Figure 4), we can confirm the view that the effect of spinning is partial dehydration of the silica surface. In fact, the spectra in Figure 4 of the unsealed sample that has been spinning for 4 or 6 h are very similar to the one that was obtained from the sample that was evacuated at 0 °C (Figure 5c); and the spectrum of the

(75) Zhdanov, S. P.; Kiselev, A. W. *Zh. Fiz. Khim.* **1957**, *31*, 2213.

(76) Morrow, B. A.; McFarlan, A. *J. Langmuir* **1991**, *7*, 1695.

(77) Zhuravlev, L. T. *Langmuir* **1987**, *3*, 316.

(78) Leonardelli, S.; Facchini, L.; Fretigny, C.; Tougen, P.; Legrand, A. *J. Am. Chem. Soc.* **1992**, *114*, 6412.

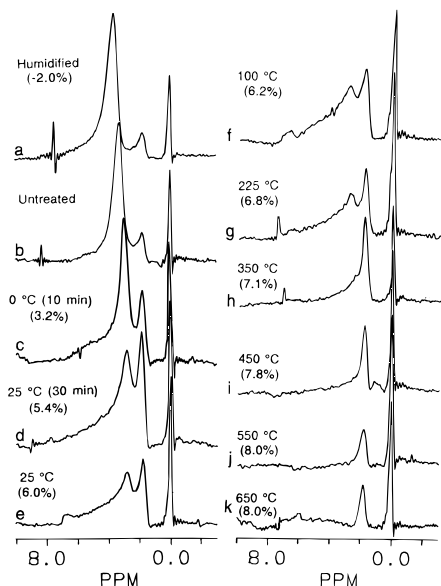


**Figure 5.**  $^1\text{H}$  CRAMPS spectra of HS-5 Cab-O-Sil (and intensity reference) that was evacuated/dehydrated at various temperatures, for 6 h unless otherwise indicated. Weight loss relative to the untreated sample is given in parentheses.

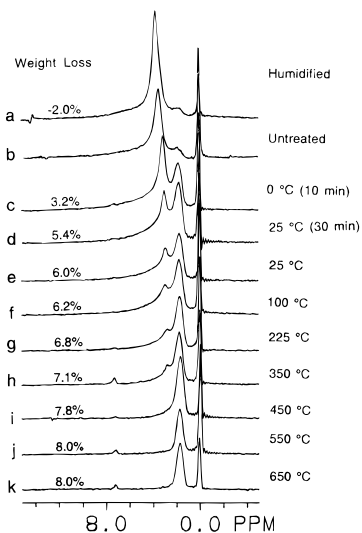


**Figure 6.**  $^1\text{H}$  MAS-only spectra of HS-5 Cab-O-Sil that has been evacuated/dehydrated (for 6 h, unless otherwise indicated) at various temperatures (with intensity reference); MAS speed is 12 kHz. Weight loss relative to the untreated sample is indicated.

sample that has been spun for 12 h (bottom spectrum in Figure 4) is similar to those of the samples dehydrated at room temperature (Figure 5, d and e). It appears that sample spinning provides a way of effecting and monitoring the gradual change of the Cab-O-Sil surface as it is dehydrated.

For undehydrated Cab-O-Sil samples (Figure 5a,b), the  $^1\text{H}$  NMR spectrum is dominated by a sharp peak at 4.1 ppm for the humidified sample and 3.5 ppm (the physisorbed water) for the untreated silica. The 4.1-ppm chemical shift is intermediate between that of liquid water protons, 4.9 ppm, and that of the physisorbed water peak in the untreated sample (3.5 ppm). It is most likely that the humidified sample has such a high water content that some of the water molecules exist as liquid-like water without any direct interaction with the silica surface. The peak position at 4.1 ppm is probably a result of rapid proton exchange between liquid water and physisorbed water.

It is worth noting that at a high hydration level, e.g., the saturated state (Figure 5a), the isolated silanol peak at 2.0 ppm

is still present in the  $^1\text{H}$  NMR spectrum of Cab-O-Sil, indicating that there are some silanol groups that cannot be hydrogen bonded to water molecules; these fumed silica silanols must be inaccessible by water molecules and are truly "isolated". This behavior is in contrast to what is observed in the silica gel case, in which even on an untreated silica gel surface, all of the silanols are hydrogen-bonded silanols (Figure 3a). This type of isolated silanol in fumed silica may be located at a point of contact between two or more particles; such silanols are referred to as interparticle silanols in this work, and will be discussed in more detail below.

Examining the spectra of Figures 5 and 6, the first observable effect of dehydration is the attenuation of the intensity of the peak at 3.5 ppm in the sample that is evacuated at 0 °C for only 10 min. This demonstrates that the physisorbed water on the Cab-O-Sil surface is very easily desorbed. The spectra obtained on a sample subjected to 25 °C evacuation for 30 min show further attenuation of intensity in the 3.5-ppm peak. This facile removal of water responsible for the peak at 3.5 ppm is behavior that one would expect for water that is physically adsorbed on the silica surface. Continuing the evacuation at 25 °C for 6 h causes the water peak to decrease slightly more; also there is only a very small decrease in weight observed. With evacuation at 100 or 225 °C, the further decrease in the physisorbed water peak intensity is very small. As discussed below, this peak is more generally assigned as labile (e.g., rapidly exchanging), weakly hydrogen-bonded hydroxyls, including those of both water and silanols.

The most dominant change in the spectra of Figures 5 and 6 over the 100–225 °C temperature range is manifested in the broadly spread intensity of the lower shielding side of the spectrum, which is reduced when the evacuation temperature is increased. This indicates that some of the very strongly hydrogen-bonded silanols start to condense with each other at temperatures of about 225 °C or higher. Since increased hydrogen-bonding strength is typically identified with decreased shielding and since the intensity at the low-shielding side of the  $^1\text{H}$  spectra is attenuated first as the evacuation temperature is increased, it appears that the stronger the hydrogen bonding between the two adjacent silanols, the more easily condensation occurs. This is understandable from the point of view of chemical mechanisms, because a condensation reaction between two silanols presumably is related to their proximity with respect to each other, which can be correlated with hydrogen-bonding interactions between them.

For the fumed silica sample evacuated at 350 °C, the hydrogen-bonded silanol intensity has decreased dramatically (Figure 5h), relative to that of the sample evacuated at 225 °C (Figure 5g). The lower-shielding side of this complex signal is eliminated completely, leaving some of the more weakly hydrogen-bonded silanols present as a shoulder of the isolated silanol peak at about 2.0 ppm. Hydrogen-bonded silanols are not completely eliminated until the dehydration temperature reaches about 450 °C. When the dehydration temperature reaches 550 or 650 °C, the  $^1\text{H}$  NMR spectra of Cab-O-Sil show little or no evidence of hydrogen-bonded silanols or water; only the isolated silanol peak at 2.0 ppm remains. From Table 3, which summarizes the experimental  $^1\text{H}$  CRAMPS results on dehydration, we see that the amount of isolated silanols on the dehydrated surface is almost the same for samples dehydrated at 550 and 650 °C.

As shown in both Figures 4 and 5, the dominant peak in the  $^1\text{H}$  spectra is gradually moved to higher shielding, as the sample is increasingly dehydrated by spinning for a longer period or by evacuation at a higher temperature, until at some temperature

**Table 3.** Summary of Total  $^1\text{H}$  CRAMPS Integral of Each Spectrum in Figure 5 and Weight Loss of the Cab-O-Sil Sample in Each Step During Dehydration

samples	weight loss (%) <sup>a</sup>	total integral <sup>b</sup>
humidified	-2.0 <sup>c</sup>	13 × 10
untreated	0	11 × 10
0 °C, 10 min	3.2	83
25 °C, 30 min	5.4	71
25 °C, 6 h	6.0	60
100 °C, 6 h	6.2	53
225 °C, 6 h	6.8	42
350 °C, 6 h	7.1	39
450 °C, 6 h	7.8	34
550 °C, 6 h	8.0	30
650 °C, 6 h	8.0	29

<sup>a</sup> All percentages are relative to the untreated sample; estimated error:  $\pm 10\%$ . <sup>b</sup> Obtained after calibration relative to the intensity standard; estimated error:  $\pm 3\%$ . <sup>c</sup> 2% weight gain from untreated sample.

above 225 °C this peak has been eliminated as a directly resolved peak. Because surface hydroxyls have been shown to be the principal sites for physisorption of water,<sup>25</sup> dehydration makes the surface progressively more hydrophobic; and the higher the hydrophobicity of the surface, the higher is the proton shielding of the hydroxyl species. One can see from the  $^1\text{H}$  NMR spectra of Figures 5 and 6 that for 100 and 225 °C (and probably 250 °C) evacuation temperatures, there is a peak at about 3.0 ppm, a chemical shift that indicates hydroxyl protons with very weak  $^1\text{H}$ - $^1\text{H}$  dipolar interactions. Since physisorbed water should be completely removed from the surface by evacuation at 225 and 350 °C, it is reasonable to assign this peak in the spectra of the samples evacuated at 225 and 350 °C to silanols with very weak hydrogen bonding. The  $^1\text{H}$ - $^1\text{H}$  dipolar interactions of these very weak hydrogen-bonded silanols must be weak enough to be substantially averaged by 2 kHz magic-angle spinning (Figure II of the supporting information).

As expected, a higher evacuation temperature facilitates a more complete dehydroxylation of interacting silanols. The sequence of surface dehydration is as follows: (a) at low temperatures the initial removal of physisorbed water and conversion of some of the hydrogen-bonded silanols, which were originally (i.e., before evacuation) hydrogen bonded only to water molecules, to isolated silanols, followed at higher temperatures by (b) the progressive removal (dehydroxylation) of strongly hydrogen-bonded silanols via condensation of water, and then (c) analogous removal of weakly hydrogen-bonded silanols via condensation/dehydroxylation. In the Cab-O-Sil case, the elimination of water that is adsorbed in the molecular form is basically complete at 25 °C under vacuum. At a temperature of 225 °C, adjacent silanol groups on the silica surface (including the hydrogen-bonded interparticle silanols at the contact points between particles) start to condense and form water. Complete condensation of hydrogen-bonded silanols on the Cab-O-Sil surface occurs at 450 °C and above. This interpretation is consistent with the conclusion given by Morrow and McFarlan, based on their IR studies.<sup>3</sup>

In the silica gel case, evacuation at 25 °C also leads to a dramatic loss of intensity at 3.5 ppm.<sup>64</sup> However, in that case the peak corresponding to hydrogen-bonded silanols remaining after removal of physisorbed water is simply a broad band instead of the sharper feature shown in the Cab-O-Sil case; i.e., a peak at 3.0 ppm is obvious in Figures 5f and 5g (and, as a shoulder, Figure 5h) in addition to the broad band underneath it. This fact probably implies that there is a different distribution of hydrogen bonding strengths and structures involved on the Cab-O-Sil surface than that on the silica gel surface. Evacuation of a silica gel sample at 500 °C removes the peak due to

hydrogen-bonded silanols, leaving only the isolated silanol peak at 1.7 ppm.<sup>64</sup> The overall sequence of dehydration of silica gel reported earlier<sup>64</sup> is very similar to what we obtained on Cab-O-Sil silica in this study: after the physisorbed water is removed from the silica surface, the hydrogen-bonded silanols start to condense with each other, with strongly hydrogen-bonded silanols condensing first (at lower temperatures), followed by weakly hydrogen-bonded silanols (at higher temperatures); isolated silanols remain on the surface after evacuation at 500–600 °C.

The concentration of silanol groups on the silica surface is an issue that has been explored since the 1960's, based on a variety of methods.<sup>2-52</sup> The silanol concentration for Aerosil, another fumed silica, is well-known to be about 3 OH/(nm)<sup>2</sup>, a value obtained by quite a few investigations.<sup>21-24</sup> Use of silicone polymer as a  $^1\text{H}$  NMR intensity standard in this Cab-O-Sil silica study provides another very useful way of calculating hydroxyl densities on surfaces.<sup>74</sup> Absolute integrated intensities of the NMR signals for a mixture consisting of known weights of silica and silicone rubber enable one to evaluate the surface densities of hydroxyls. Based on information derived from spectra such as those in Figures 5f and 6f, from the integral ratio of the Cab-O-Sil silica and silicone rubber signals and from the known surface area (325 m<sup>2</sup>/g) of the Cab-O-Sil silica, the concentration of silanol groups on a HS-5 Cab-O-Sil sample from which physisorbed water has been removed is found to be  $2.8 \pm 0.3$  OH/(nm)<sup>2</sup>, which is in good agreement with the corresponding results obtained by other techniques.<sup>21-24</sup>

**$^1\text{H}$  CRAMPS Spin-Lattice Relaxation.** In favorable cases, measurement of the  $^1\text{H}$  spin-lattice relaxation time of a solid sample can provide information on atomic level mobility and/or on the extent of spin communication between different proton spin sets that are resolvable in the spectrum of the sample. Spin communication can occur either by chemical exchange<sup>79</sup> or by spin diffusion,<sup>80</sup> both of which are chemically relevant from dynamic/structural points of view. Spin diffusion is a process by which resolvable spin sets achieve thermal equilibrium with respect to each other, following a perturbation of the system that leaves the different spin sets in different states of nuclear spin polarization. This equilibration process can occur via (a) mutual spin-spin flip-flops, which are based on dipolar interactions (which in turn depend on atomic-level structure and dynamics), and (b) chemical (i.e., proton) exchange.

Proton  $T_1$  measurements, based on a Freeman-Hill version of the CRAMPS-detected inversion-recovery technique,<sup>69</sup> were carried out on an untreated Cab-O-Sil HS-5 sample and on a corresponding sample evacuated for 6 h at 25 °C. In the results on both samples, all peaks and shoulders appeared to relax according to a common exponential term. For the untreated sample, the measured  $^1\text{H}$   $T_1$  value is  $340 \pm 15$  ms, and for the 25 °C evacuated sample,  $680 \pm 30$  ms. The fact that only one  $^1\text{H}$   $T_1$  value is observed for each sample implies that spin exchange, by spin-spin flip-flops and/or chemical exchange, occurs between the different spin sets that can be distinguished via chemical shifts on a time scale that is short compared to  $\sim 0.5$  s. The fact that  $T_1^{\text{H}}$  for the untreated sample is roughly half that of the 25 °C evacuated sample is reasonable, as one expects spin-lattice relaxation to be more efficient for the protons of relatively mobile physisorbed water than for silanol protons; and the physisorbed water contribution to the spin-exchange averaged  $T_1^{\text{H}}$  values observed is larger for the untreated sample.

(79) Kaplan, J. I.; Fraenkel, G. *NMR of Chemically Exchanging Systems*; Academic: New York, 1980.

(80) Goldman, M. *Spin Temperature and Nuclear Magnetic Resonance in Solids*; Clarendon: Oxford, 1970.

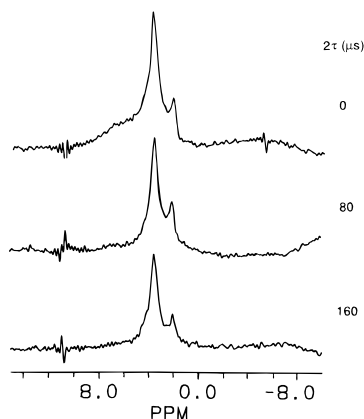


**Figure 7.**  $^1\text{H}$  CRAMPS dipolar-dephasing<sup>69</sup> results on an untreated HS-5 Cab-O-Sil sample.

**Dipolar-Dephasing Experiment.** Confirmation of the  $^1\text{H}$  peak assignments given above and additional information on the relationship between the two types of silanol moieties (hydrogen-bonded silanols and isolated silanols) can be obtained by direct observation of their transverse relaxation behaviors in a dipolar-dephasing experiment.<sup>69</sup> In this experiment, the dipolar dephasing that occurs during the period that precedes BR-24 detection preferentially attenuates the transverse magnetization of the protons that are most strongly involved in dipolar interactions with other protons. Experimental results obtained by this technique on an untreated Cab-O-Sil sample are shown in Figure 7. The spectra show that, after 80  $\mu\text{s}$  of dipolar dephasing, the broad peak from 1 to 8 ppm is essentially gone, a behavior consistent with the interpretation that this peak is due to silanol protons involved in strong dipolar interactions, as would be expected in hydrogen-bonding situations. In contrast, very little of the intensities at 3.5 and 2.0 ppm have decayed after 80  $\mu\text{s}$ . This lack of dephasing is indicative of very weak  $^1\text{H}$ – $^1\text{H}$  dipolar interactions, which is a result of the high mobility of physisorbed water and the “isolation” of the 2-ppm silanols on the silica surface, which attenuate  $^1\text{H}$  dipolar interactions. The  $^1\text{H}$ – $^1\text{H}$  dipolar coupling between isolated silanol protons is weakened by large  $^1\text{H}$ – $^1\text{H}$  internuclear distances and/or partially averaged by rotation of hydroxyl groups around the Si–OH axis (*vide infra*). These results are reminiscent of what has been published previously on silica gel.<sup>69</sup>

**$^1\text{H}$  Spin-Exchange Experiment.** The third type of  $^1\text{H}$  CRAMPS relaxation experiment that we have employed to examine this system is one designed to display spin exchange directly.<sup>69</sup> The spin-exchange experiment utilized here initially establishes a magnetization gradient through dipolar dephasing to select one “type” of proton. The dephasing period was chosen to be long enough (80  $\mu\text{s}$ ) that magnetization of rapidly-dephasing components decays away, but short enough that net magnetization in a slowly-decaying component is preserved. Following the dephasing period, the selected protons retain a net magnetization that is then stored along the longitudinal axis during a variable “mixing period”, in which the stored magnetization is allowed to exchange with nearby spins via  $^1\text{H}$ – $^1\text{H}$  dipolar couplings and chemical exchange. The resulting magnetization, following exchange, is detected via CRAMPS. If spin exchange occurs, the magnetization of the initially selected spins decreases, as magnetization is shared with and builds up in the unselected protons.

In the present case, a dipolar-dephasing time of 80  $\mu\text{s}$  ( $2\tau$ ) was employed to greatly diminish the  $^1\text{H}$  spin polarization of the strongly coupled, hydrogen-bonded silanol protons, leaving

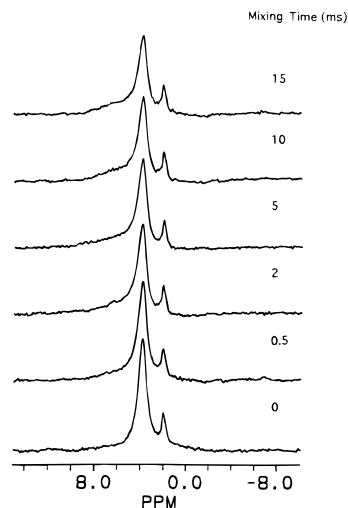


**Figure 8.**  $^1\text{H}$  CRAMPS spin exchange<sup>69</sup> results on an untreated HS-5 sample, obtained using a dipolar-dephasing time of 80  $\mu\text{s}$ .

the polarizations of physisorbed water and isolated silanol protons only slightly attenuated (see Figure 7) and therefore being *selected* during the dipolar-dephasing period. Figure 8 displays the results of the  $^1\text{H}$  CRAMPS spin-exchange experiment carried out on an untreated HS-5 Cab-O-Sil sample. For a zero mixing time, the result is essentially the same as that obtained in the dipolar dephasing experiment with  $\tau = 80 \mu\text{s}$  (Figure 7). One can see from Figure 8 that the low-shielding, broad peak starts to appear after a mixing time of 0.5 ms, and a higher degree of equilibration occurs by 5 ms of mixing time.

When each of the spectra shown in Figure 8 was deconvoluted, the corresponding deconvolution/simulation results (not given here)<sup>73</sup> show that, as the resonance due to hydrogen-bonded silanol protons becomes more and more intense (increasing mixing time), the physisorbed water peak intensity is decreased. The isolated silanol peak intensity is almost unchanged. This implies that spin exchange between the hydrogen-bonded silanol protons and physisorbed water protons is much more efficient than that between the two types of silanol protons. Since some of the hydrogen-bonded silanols are actually hydrogen bonded to water molecules, this relative efficiency of exchanges is not surprising. The isolated silanols are mainly surrounded by siloxane bonds and/or located in some inaccessible sites, like interparticle contacts (*vide infra*). The overall patterns seen in Figures 7 and 8 are reminiscent of behavior reported previously for silica gel.<sup>69</sup> From the experimental results shown in Figure 8, it appears that spin exchange of the physisorbed water protons with hydrogen-bonded silanol protons occurs on a time scale of 1–10 ms, while with isolated silanols there is no substantial spin exchange in 15 ms. However, the fact that a common  $T_1^{\text{H}}$  value of about 200 ms was measured for all of the protons in this sample implies that spin exchange between hydrogen-bonded and non-hydrogen-bonded silanol protons is fast relative to 200 ms. This pattern is consistent with the surface model discussed below.

**$^{29}\text{Si}$  CP/MAS.** As the vast majority of protons in Cab-O-Sil silica particles are on the surface, the  $^{29}\text{Si}$  NMR spectra of these materials obtained by  $^1\text{H}$ – $^{29}\text{Si}$  CP are dominated by surface silicon nuclei. In 1980, Maciel and Siefert published the first example of the use of  $^1\text{H}$ →X cross polarization for surface-selective observation of a nucleus X in a demonstration of  $^1\text{H}$ – $^{29}\text{Si}$  CP in silica gel.<sup>57</sup> Since that time  $^1\text{H}$ – $^{29}\text{Si}$  CP has remained the most popular application of this surface-selective strategy, although there has also been significant success with applications to other types of systems.



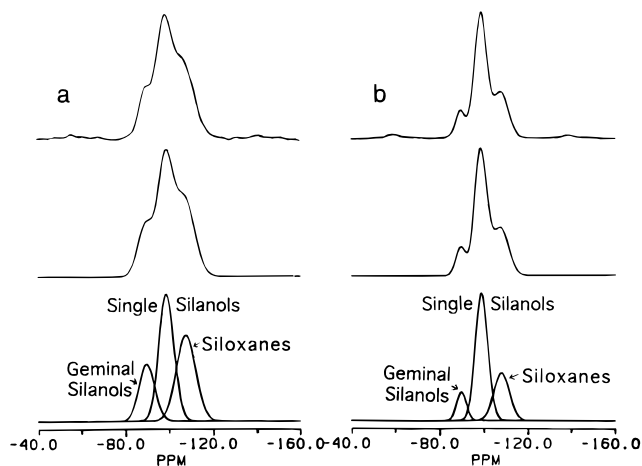


**Figure 9.**  $^{29}\text{Si}$  CP-MAS NMR spectra of (a) untreated HS-5 Cab-O-Sil (3600 scans) and (b) untreated silica gel (504 scans). CP contact time 5 ms; repetition delay 1 s. Each set of spectra includes the experimental spectrum (top), the simulated spectrum (middle), and the individual contributions to the simulated spectrum (bottom).

Various Cab-O-Sil samples were examined using a variety of  $^{29}\text{Si}$  CP-MAS NMR techniques. In order to make comparisons, some experiments were also carried out on silica gel in this study, and are presented here. The  $^{29}\text{Si}$  CP-MAS spectra of untreated Cab-O-Sil (HS-5) and silica gel (S-679) are shown in Figure 9, together with the corresponding computer simulated spectra (95% Gaussian, 5% Lorentzian) and their individual deconvoluted contributions from each silicon site. The two silica samples represented in Figure 9 were kept together in a closed chamber for 10 days, in order to establish a moisture equilibration between them. Both experimental spectra were obtained by using a CP contact time of 5 ms.

The  $^{29}\text{Si}$  CP-MAS spectra of Cab-O-Sil in Figure 9 illustrate the well-established features seen in the  $^{29}\text{Si}$  NMR spectra of silica gel,<sup>57</sup> although broadened in the Cab-O-Sil case. The peak at  $-89$  ppm is attributed to silicon atoms that have two hydroxyl groups attached,  $(\text{Si}-\text{O})_2\text{Si}(\text{OH})_2$ , often referred as  $\text{Q}_2$  silicons or as geminal silanols. The resonance at  $-99$  ppm is due to silicons with only one hydroxyl group (single silanol),  $(\text{Si}-\text{O})_3\text{Si}-\text{OH}$  ( $\text{Q}_3$ ). Any  $\text{Q}_4$  silicons,  $\text{Si}(\text{O}-\text{Si})_4$ , that can be cross polarized by nearby protons give rise to the peak at  $-109$  ppm. These assignments can be made on the basis of the usual kinds of empirical chemical shift correlations with structure from liquid-sample data on silicic acid solutions.<sup>81</sup> However, the dynamics of the  $^1\text{H}-^{29}\text{Si}$  CP process can also be used to make these assignments. The peak at  $-109$  ppm indicates that the  $\text{Q}_4$  silicons, which are not chemically bonded to any hydroxyl group(s), are observable. As the dipolar interaction responsible for the CP enhancement decreases rapidly as a function of the distance between  $^1\text{H}$  and  $^{29}\text{Si}$ , these observable  $\text{Q}_4$  silicons are in the neighborhood of silanol groups.

It is obvious in Figure 9 that all three types of silicon sites ( $\text{Q}_2$ ,  $\text{Q}_3$ ,  $\text{Q}_4$ ) in fumed silica have larger  $^{29}\text{Si}$  line widths than those in the silica gel spectrum. This greater line width presumably relates to the greater dispersion of local surface geometries (and isotropic chemical shifts) in the Cab-O-Sil surface, which is formed at much higher temperatures. This peak broadening is seen explicitly for the  $\text{Q}_4$  peak that is obtained without cross polarization (MAS-only, with  $^1\text{H}$  decoupling), i.e., with direct polarization (DP-MAS) via  $^{29}\text{Si}$  spin-lattice relaxation, as seen for the same Cab-O-Sil and silica gel samples in Figure 10. These spectra are dominated by the  $^{29}\text{Si}$

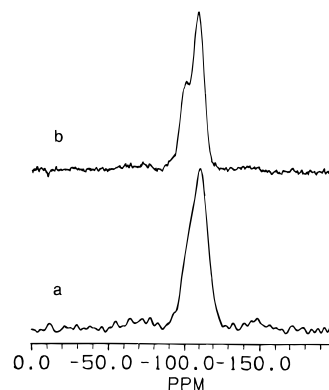


**Figure 10.**  $^{29}\text{Si}$  DP-MAS NMR spectra of (a) untreated HS-5 Cab-O-Sil (400 scans) and (b) untreated silica gel (80 scans). Repetition delay 120 s.

**Table 4.** Parameters Derived for Deconvoluted Peaks of the  $^{29}\text{Si}$  CP-MAS Spectra of Untreated Cab-O-Sil and Silica Gel (Figure 9)

sample	peak <sup>a</sup>	LW <sub>HM</sub> <sup>b</sup> ( $\times 10^{-1}$ Hz)	peak area <sup>c</sup>	$\text{Q}_2:\text{Q}_3$	$\text{Q}_2:(\text{Q}_2 + \text{Q}_3)$
Cab-O-Sil	$\text{Q}_2$	37	33	1.0:2.1	1.0:3.1
	$\text{Q}_3$	35	70		
	$\text{Q}_4$	45	61		
silica gel	$\text{Q}_2$	23	10	1.0:6.0	1.0:7.0
	$\text{Q}_3$	30	60		
	$\text{Q}_4$	36	28		

<sup>a</sup>  $\text{Q}_2$ : geminal silanol.  $\text{Q}_3$ : single silanol.  $\text{Q}_4$ : siloxane. <sup>b</sup> Line width at half maximum; estimated error:  $\pm 3\%$ . <sup>c</sup> Arbitrary units; estimated error:  $\pm 5\%$ .

line shape of  $\text{Q}_4$  sites, because the  $^{29}\text{Si}$  DP-MAS experiment more faithfully represents the bulk (internal) silicons, instead of the surface silicons that are emphasized by cross polarization because of proximity to protons.

As seen in Figure 10,  $\text{Q}_4$  silicons in Cab-O-Sil silica have a wide distribution of chemical shifts, rendering the silanol peaks directly unresolvable (without deconvolution) in the DP-MAS spectrum. Nevertheless, the single silanol peak is clearly present as a distinct shoulder on the  $\text{Q}_4$  peak in the DP-MAS spectrum of silica gel. The origin of the larger line width in the Cab-O-Sil case is related to variations in site geometry, e.g., to variations of the  $\text{Si}-\text{O}-\text{Si}$  angle between adjacent  $\text{Q}_4$  tetrahedra,<sup>29,82</sup> and possibly to variations in  $\text{Si}-\text{O}$  bond lengths. This extensive variation probably occurs in Cab-O-Sil because it is produced at high temperatures, from which more highly strained bonds can be locked in upon rapid cooling, in contrast to silica gels, which are prepared at much lower temperatures.

Table 4 summarizes the deconvoluted peak areas and line widths of the spectra in Figure 9. Results from a CP experiment using only one CP contact time do not *a priori* provide quantitative information, because the intensities in CP spectra are affected by the details of CP dynamics. Therefore, the deconvoluted peak areas presented in Table 4 for each peak in both Cab-O-Sil and silica gel spectra were calculated after compensation for differences in CP and  $^1\text{H}$  spin-lattice relaxation dynamics, the CP dynamics being determined by variable contact-time experiments (*vide infra*).

Aside from the line width difference, the main difference found between the  $^{29}\text{Si}$  CP-MAS spectra of silica gel and Cab-O-Sil is the intensity ratio of single-silanol to geminal-silanol peaks, which is about 2.1 for Cab-O-Sil and 6.0 for silica gel, after compensation for CP dynamics. The ratios of populations of geminal sites to total silanol sites (single and geminal silanols) are also presented in Table 4. Differences in the population

(81) Marsmann, H. C. Z. *Naturforsch. B.* **1974**, *29*, 495.

(82) Dupree, E.; Pettifer, R. F. *Nature* **1983**, *308*, 523.

ratios of these two kinds of silanols constitute very substantial chemical structural differences between these two kinds of silica.

**Variable Contact-Time (VCT) Experiments.** The usual approach for characterizing CP dynamics is based on the analysis of variable contact-time data in terms of eq (1):<sup>83</sup>

$$M(t) = \frac{M^\infty}{1 - T_{1\rho}^H/T_{SiH}} \{ \exp(-t/T_{1\rho}^H) - \exp(-t/T_{SiH}) \} \quad (1)$$

In this equation, which is valid for the case  $T_{1\rho}^{Si} \gg T_{1\rho}^H$  and  $T_{SiH}$ , and with  $^{29}\text{Si}$  present at only 4.7% in natural abundance,  $t$  is the variable CP contact time, and  $M^\infty$  is the  $^{29}\text{Si}$  intensity that would be achieved if  $T_{1\rho}^H$  and  $(T_{SiH})^{-1}$  were both infinite;  $T_{1\rho}^H$  is the proton spin-lattice relaxation time in the rotating frame of the applied radio frequency field.  $T_{SiH}$  is the cross-polarization time constant that represents the coupling between the  $^{29}\text{Si}$  spin reservoir and  $^1\text{H}$  spin reservoir. Other things (i.e., motional effects) being equal, the stronger the  $^1\text{H}$ - $^{29}\text{Si}$  dipolar interaction, the smaller the  $T_{SiH}$  value. Since a net (time-averaged) dipolar interaction depends not only on internuclear distance but also on motion of the spin sets,  $T_{SiH}$  also reflects motion in the spin systems.

In the variable contact-time strategy, values of  $T_{SiH}$ ,  $T_{1\rho}^H$ , and  $M^\infty$  are typically derived for each major peak in the  $^{29}\text{Si}$  spectra by fitting the deconvoluted intensities of a variable contact-time experiment to eq 1, using a nonlinear least-squares fit. For the silica gel system, the VCT data can be fit to eq 1 quite well with one value of  $T_{1\rho}^H$  and one value of  $T_{SiH}$  for each of the three  $^{29}\text{Si}$  peaks.<sup>67</sup> However, the VCT data of Cab-O-Sil cannot be fit directly to eq 1 with only one pair of relaxation parameters for each  $^{29}\text{Si}$  peak. From the  $^1\text{H}$  NMR study described earlier, we know that there are hydrogen-bonded and non-hydrogen-bonded silanols, corresponding to rigid and mobile regions on the silica surface, respectively. The protons of hydrogen-bonded silanols experience stronger  $^1\text{H}$ - $^1\text{H}$  dipolar interactions than those of non-hydrogen-bonded silanols. Therefore, the silicon nuclei that are attached to the two types of protons would be expected to manifest not only different  $^1\text{H}$ - $^{29}\text{Si}$  dipolar interactions but also different  $^1\text{H}$ - $^{29}\text{Si}$  spin dynamics. Hence, it is reasonable to assume two  $T_{SiH}$  values for each type of silanol on the Cab-O-Sil surface. Since only one  $T_{1\rho}^H$  value was found for these two systems from independent  $T_{1\rho}^H$  measurements (not shown here),<sup>73</sup> the following equation was used to fit the VCT data of various Cab-O-Sil samples:

$$M(t) = \frac{\beta M^\infty}{(1 - T_{1\rho}^H/T_{SiHF})} \{ \exp(-t/T_{1\rho}^H) - \exp(-t/T_{SiHF}) \} + \frac{(1 - \beta) M^\infty}{(1 - T_{1\rho}^H/T_{SiHS})} \{ \exp(-t/T_{1\rho}^H) - \exp(-t/T_{SiHS}) \} \quad (2)$$

In this equation, there are two components of  $T_{SiH}$  for each peak,  $T_{SiHF}$  and  $T_{SiHS}$ , representing the fast and slow component with respect to the cross-polarization rate, respectively. The parameter  $\beta$  is the fraction of the fast-CP component for a given  $^{29}\text{Si}$  peak; correspondingly,  $1 - \beta$  is the fraction of the slow-CP component.

Variable contact-time experiments were carried out on untreated samples of three grades of Cab-O-Sil silicas with different surface areas in order to investigate the role of surface area on the surface structure. Ordinarily the surface structure

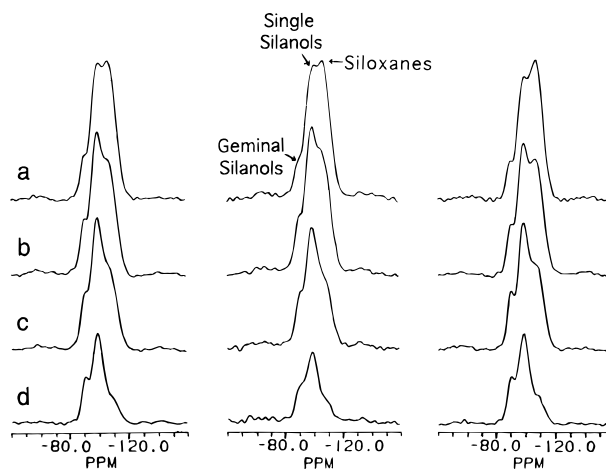


**Figure 11.**  $^{29}\text{Si}$  CP-MAS spectra of three grades of untreated Cab-O-Sil (left, HS-5 (830 mg, 3600 scans); middle, M-5 (633 mg, 8000 scans); right, L-90 (830 mg, 15000 scans) with four CP contact times: (a) 20 ms, (b) 10 ms, (c) 5 ms, and (d) 1 ms.

is closely related to the size of individual silica globules and the arrangement of elementary silica particles in their formation. Figure 11 shows representative  $^{29}\text{Si}$  CP-MAS spectra, obtained with four different CP contact times, on HS-5, M-5, and L-90 Cab-O-Sil silicas. One can see that the spectra from these three Cab-O-Sil silicas display very similar features, but some differences in detail. The curves representing the fitting of deconvoluted peak intensities<sup>67</sup> from the VCT experiments to eq 2 for the three silicon sites of the three Cab-O-Sil samples are shown in Figure 12. The derived values of  $T_{SiH}$  and  $M^\infty$  are listed in Table 5, along with the independently-determined  $T_{1\rho}^H$  values and  $T_1^H$  values (obtained via CP-based  $^{29}\text{Si}$ -detection experiments not shown here).<sup>73</sup>

For each of the three untreated samples, two components of  $T_{SiH}$  were found for each peak, as shown in Table 5. About 38–45% of the single-silanol peak has a  $T_{SiH}$  value on the order of 0.5–0.7 ms; the remaining component of the single-silanol intensity cross polarizes with a much larger  $T_{SiH}$  value of about 6–14 ms. Similar results were obtained for the geminal silanols, except there is a larger fraction (57–72%) of the  $T_{SiHF}$  component than that for the single silanols.

The CP time constant is roughly a measure of the inverse of the square of the magnitude of the  $^1\text{H}$ - $^{29}\text{Si}$  dipolar interaction.<sup>84</sup> Hence, the slow component of  $T_{SiH}$  ( $T_{SiHS}$ ) presumably corresponds to much weaker  $^1\text{H}$ - $^{29}\text{Si}$  dipolar interactions compared to the fast  $T_{SiH}$  component ( $T_{SiHF}$ ). The silanols with a 0.5–0.7-ms  $T_{SiH}$  value can be attributed to hydrogen-bonded single and geminal silanols, since hydrogen bonding favors cross polarization from proton to silicon atoms by presenting (a) a larger number of protons available for cross polarizing a specific silicon nucleus and (b) less motional averaging of each  $^1\text{H}$ - $^{29}\text{Si}$  dipolar interaction. Those silanols with a larger  $T_{SiH}$  value (6–14 ms) are identified as not hydrogen bonded, for both single and geminal silanols.

Evidence for rotation or torsional oscillation of the OH group about the Si-OH bond of silica was presented by Peri.<sup>52</sup> If a silanol hydroxyl group experiences only weak (at most) or no hydrogen bonding, it is possible that it rotates around the Si-OH axis rapidly enough to substantially average the  $^1\text{H}$ - $^{29}\text{Si}$  dipolar interactions. The rotational averaging effect will result in a larger  $T_{SiH}$ , which can give rise to the slow component ( $T_{SiHS}$ ) in this study. Since both single and geminal silanols have two  $T_{SiH}$  components, there must be hydrogen-bonded

(83) Mehring, M. *NMR, Basic Principles and Progress*; Springer Verlag: Berlin Heidelberg, New York, 1976; p 138.

(84) Slichter, C. P. *Principles of Magnetic Resonance*, 3rd ed.; Springer-Verlag: New York, 1989; p 79.

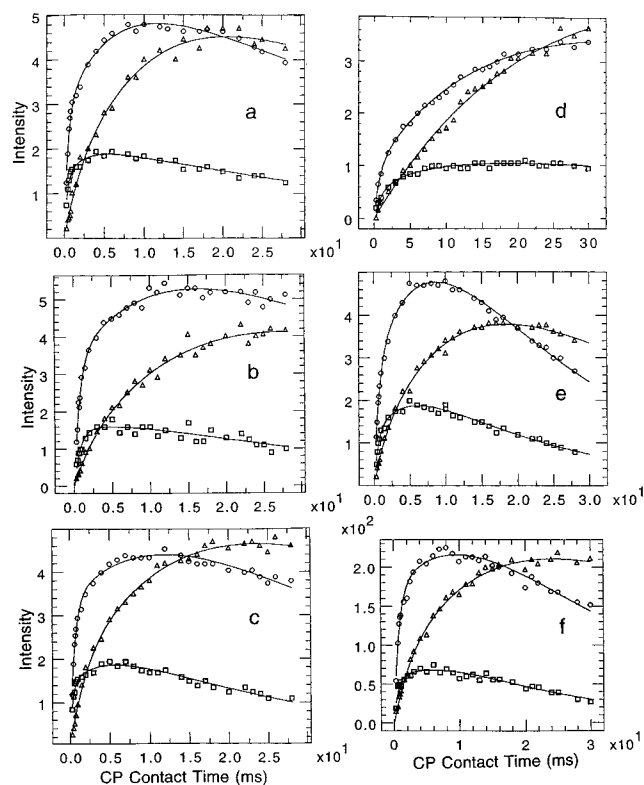


**Figure 12.**  $^{29}\text{Si}$  CP-MAS variable contact-time (VCT) data and fitting curves. (a) Single silanol (O), geminal silanol (□), and siloxane ( $\Delta$ ) peaks of untreated HS-5 Cab-O-Sil; (b) Single silanol (O), geminal silanol (□), and  $\text{Q}_4$  ( $\Delta$ ) peaks of untreated M-5 Cab-O-Sil; (c) Single silanol (O), geminal silanol (□), and  $\text{Q}_4$  ( $\Delta$ ) peaks of untreated L-90 Cab-O-Sil; (d) Single silanol (O), geminal silanol (□), and  $\text{Q}_4$  ( $\Delta$ ) peaks of HS-5 Cab-O-Sil dehydrated at  $200^\circ\text{C}$  and  $10^{-3}$  Torr; (e) Single silanol (O), geminal silanol (□), and  $\text{Q}_4$  ( $\Delta$ ) peaks of water-treated HS-5 Cab-O-Sil; (f) Single silanol (O), geminal silanol (□), and  $\text{Q}_4$  ( $\Delta$ ) peaks of water-treated M-5 Cab-O-Sil.

**Table 5.** Relaxation Time Constants and Relative Contributions for Various Cab-O-Sil Samples Determined by  $^{29}\text{Si}$  CP-MAS NMR

sample	peak	$T_{1\rho}^{\text{H}}$ (ms) <sup>a</sup>	$T_{\text{SiHF}}$ (ms) <sup>a</sup>	$\beta$ (%) <sup>a</sup>	$T_{\text{SiHS}}$ (ms) <sup>a</sup>	$T_1^{\text{H}}$ (s) <sup>b</sup>
HS-5	$\text{Q}_2$	54	0.42	62	3.4	0.22
	$\text{Q}_3$		0.53	45	6.0	
	$\text{Q}_4$		1.5	10	11	
M-5	$\text{Q}_2$	40	0.81	72	8.1	0.22
	$\text{Q}_3$		0.70	38	14	
	$\text{Q}_4$		1.8	15	18	
L-90	$\text{Q}_2$	30	0.40	57	5.4	0.23
	$\text{Q}_3$		0.62	42	13	
	$\text{Q}_4$		2.0	14	23	
HS-5( $\text{H}_2\text{O}$ ) <sup>c</sup>	$\text{Q}_2$	20	0.50	41	5.0	0.21
	$\text{Q}_3$		0.68	35	7.9	
	$\text{Q}_4$		1.5	7.4	20	
M-5( $\text{H}_2\text{O}$ ) <sup>d</sup>	$\text{Q}_2$	21	0.61	37	6.6	0.17
	$\text{Q}_3$		0.78	26	12	
	$\text{Q}_4$		0.71	3.0	25	
M-5( $\text{D}_2\text{O}$ ) <sup>e</sup>	$\text{Q}_2$	$11 \times 10$	0.35	24	15	0.45
	$\text{Q}_3$		0.52	16	17	
	$\text{Q}_4$		1	1	25	

<sup>a</sup> Estimated error:  $\pm 10\%$ . <sup>b</sup> Estimated error:  $\pm 5\%$ . <sup>c</sup> See Experimental Section for preparation. <sup>d</sup> See Experimental Section for preparation. <sup>e</sup> See Experimental Section for preparation. <sup>f</sup> Two  $T_1^{\text{H}}$  components, with weight fractions of 0.70 for 0.42 s and 0.30 for 2.0 s.

single and geminal silanols, as well as isolated single and geminal silanols on the Cab-O-Sil surface. As shown in Table 5, the geminal silanols have a much lower  $T_{\text{SiHS}}$  value than that of the single silanols. This is most likely the result of both factors (a) and (b) stated above, as well as the fact that there

are two OH groups, rather than one, attached to a geminal silicon. One expects little rotational motion of geminal silanols due to hydrogen bonding between two hydroxyl groups attached to adjacent silicon atoms.<sup>70</sup> In contrast to rotating isolated single silanols, the more rigid hydrogen-bonded silanols in Cab-O-Sil silica would experience larger, less rotationally-averaged  $^1\text{H}$ – $^{29}\text{Si}$  dipolar interactions, resulting in a correspondingly smaller  $T_{\text{SiHF}}$  value.

We can see in Table 5 that  $T_{\text{SiHS}}$  values of single and geminal silanols are roughly 15 times larger than the corresponding  $T_{\text{SiHF}}$  values. Because  $T_{\text{SiHF}}$  and  $T_{\text{SiHS}}$  are identified with the hydrogen-bonded silanols and isolated silanols, respectively, as discussed above, this ratio implies that the hydrogen-bonded silanols experience net  $^1\text{H}$ – $^{29}\text{Si}$  dipolar interactions that are approximately four times as strong as those seen for isolated silanols. Besides the factor of rotational motion of isolated single-silanol hydroxyl groups, there is also a factor due to the fact that hydrogen-bonded silanols are relatively rigidly bonded to water molecules and other neighboring silanols, and the protons of these nearby moieties also contribute to the  $^1\text{H}$ – $^{29}\text{Si}$  dipolar interaction of the silicons of hydrogen-bonded silanols. The  $^{29}\text{Si}$  nuclei of isolated silanols experience proton dipolar interactions mainly with their own hydroxyl protons.

The results summarized in Table 5 show that the fraction of the fast component of  $T_{\text{SiH}}$  for geminal silanols is larger than that for single silanols, indicating that most of the geminal silanols are hydrogen bonded. This result is close to a conclusion that was made in a previous report, in which Callas and co-workers<sup>5</sup> claimed that all geminal silanols on fumed silicas are hydrogen bonded.

Only a small percentage of  $\text{Q}_4$  silicons manifest a very small  $T_{\text{SiH}}$  value, and this value is usually larger than the  $T_{\text{SiHF}}$  values of silanols. Most of the  $\text{Q}_4$  silicons have a  $T_{\text{SiH}}$  value of 10–25 ms, because  $\text{Q}_4$  silicons are usually farther away from the available protons than are the silanol silicon atoms. As reported semiquantitatively for silica gel several years ago,<sup>58</sup> this observation also supports the assignment of the  $^{29}\text{Si}$  peak at  $-109$  ppm to  $\text{Q}_4$  silicons.

**“Interparticle Silanols”.** In the untreated silica gel case, all the surface silanols are hydrogen bonded, either to the hydroxyl groups of adjacent silanols or to water molecules. For silica gel, isolated (non-hydrogen bonded) surface silanols are present only in dried samples. In order to examine in more detail the fate of the isolated silanols that are found in the untreated Cab-O-Sil silica when additional water is adsorbed, variable contact-time experiments were also carried out on water-treated Cab-O-Sil samples. After fitting the experimental data to eq 2, the derived parameters, including  $T_{1\rho}^{\text{H}}$  values obtained independently,<sup>73</sup> are tabulated in Table 5 for HS-5( $\text{H}_2\text{O}$ ) and M-5( $\text{H}_2\text{O}$ ) samples.

As shown in Table 5, for the two water-treated samples, HS-5( $\text{H}_2\text{O}$ ) and M-5( $\text{H}_2\text{O}$ ), two  $T_{\text{SiH}}$  values are still needed to fit the data for single and for geminal silanols, as in the case of the untreated samples. One of the  $T_{\text{SiH}}$  values ( $T_{\text{SiHS}}$ ) for these water-treated samples is in the range of 5–12 ms, which was attributed above to isolated silanols. This result indicates that some isolated silanols are still present on the water-saturated Cab-O-Sil silica surface, i.e., are not hydrogen bonded to water molecules. The existence of isolated silanols on the water-saturated fumed silica surface suggests that the isolated silanols are located at some inaccessible sites and not available for hydrogen bonding with water molecules. This conclusion is also supported by the  $^1\text{H}$  NMR data, which show that a 2-ppm peak is present in the  $^1\text{H}$  NMR spectrum of a water-saturated sample (Figure 5). These isolated and inaccessible silanol sites

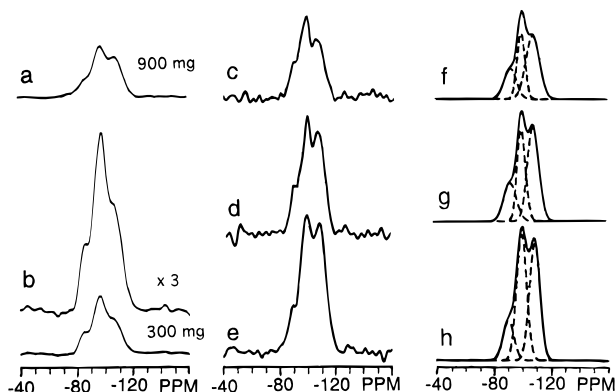


**Figure 13.**  $^{29}\text{Si}$  CP-MAS spectra of (a)  $\text{D}_2\text{O}$ -exchanged M-5 Cab-O-Sil (40 000 repetitions; 5 ms CP contact time; 6 s repetition delay; 900 mg sample); (b) Untreated M-5 Cab-O-Sil (40 000 repetitions; 5 ms CP contact time; 0.6 s repetition delay; 300 mg sample); (c–e)  $\text{D}_2\text{O}$ -exchanged Cab-O-Sil, with three repetition delays, 0.6 s (c), 3.0 s (d), and 10 s (e); (f–h) computer simulation/deconvolutions of (c), (d), and (e).

are most likely to be in the contact area between two adjacent Cab-O-Sil silica particles. These so-called *interparticle silanols* may constitute a significant fraction of the silanol groups on the Cab-O-Sil surface, because the particle size of this type of silica is known to be very small (10–20 nm for secondary particles and 1–2 nm for primary particles).<sup>85</sup> This small particle size is the reason why this non-porous material has a high surface area, and the reason why the contact area should constitute a larger fraction of the total surface area than would be the case for larger particles, e.g., for silica gel.

The results summarized in Table 5 for the water-saturated samples indicate that isolated interparticle silanols can exist as single silanols and as geminal silanols, since a substantial  $T_{\text{SiH}}$  component was found for both types of silanols. Interparticle silanols can presumably be perturbed to some extent by the interparticle contacts, and hydrogen bonding may take place between some silanols on two adjacent silica globules. This interparticle hydrogen bonding could be very strong or very weak, depending on the O–H...O distance, and such hydrogen bonding may be primarily responsible for the forces of adhesion that hold secondary particles together. If the interparticle silanols are largely inaccessible to  $\text{H}_2\text{O}$  molecules, it would be expected that deuterium exchange with  $\text{D}_2\text{O}$  molecules would not be facile. Therefore,  $\text{D}_2\text{O}$  exchange experiments would seem useful for finding out not only about internal silanols, as examined previously for silica gel,<sup>68</sup> but also about interparticle silanols.

As was previously reported,  $^{29}\text{Si}$  CP-MAS NMR intensity is depleted dramatically in a  $\text{D}_2\text{O}$ -exchanged silica gel sample.<sup>6,67</sup> It was also reported that almost all of the SiOH groups remaining after  $\text{D}_2\text{O}$  exchange are single silanols.<sup>67</sup> Figure 13 shows the  $^{29}\text{Si}$  CP-MAS spectra of untreated Cab-O-Sil and  $\text{D}_2\text{O}$ -exchanged Cab-O-Sil (M-5). These spectra clearly reveal that a significant portion (about 32%) of the silanols are highly resistant to  $\text{D}_2\text{O}$  exchange. In contrast to  $\text{D}_2\text{O}$ -exchanged silica gel, the spectrum of  $\text{D}_2\text{O}$ -exchanged Cab-O-Sil shows clearly the presence of geminal silanols. In order to quantify the extent of deuterium exchange,  $T_1^{\text{H}}$  and cross-polarization dynamics of the  $^{29}\text{Si}$  CP-MAS experiment for the  $\text{D}_2\text{O}$ -exchanged sample must be considered. The results of acquiring these data are included in Table 5.

Instead of the common  $T_1^{\text{H}}$  value of 0.22 s found for all the  $^{29}\text{Si}$  peaks in  $^{29}\text{Si}$ -CP-detected  $T_1^{\text{H}}$  experiments on untreated

Cab-O-Sil samples, for the  $\text{D}_2\text{O}$ -exchanged M-S sample two  $T_1^{\text{H}}$  components were found for the single silanol peak at –99 ppm: one is about 0.42 s, and the other is 2.0 s. This indicates that there are two regions of mobility in the system: one, the 2.0-s component, must be due to internal single silanols; and the other one is due to nonexchangeable external single silanols (i.e., interparticle single silanols) with a  $T_1^{\text{H}}$  value (0.42 s) that is close to that of the untreated sample (0.20–0.25 s). However, only one  $T_1^{\text{H}}$  value is observed for the geminal silanols at –89 ppm in the  $\text{D}_2\text{O}$ -exchanged sample represented in Figure 13a, which implies that there are no internal geminal silanols in Cab-O-Sil silica. The presence of two distinct  $T_1^{\text{H}}$  values for the single silanol protons in  $\text{D}_2\text{O}$ -exchanged Cab-O-Sil indicates that  $^1\text{H}$  spin exchange between the two corresponding spin reservoirs is very inefficient on a time scale of hundreds of ms.

The fast component of  $T_{\text{SiH}}$  listed in Table 5 for the untreated sample (Table 5), with a time constant of less than 1 ms, still exists in both the single and geminal silanols of  $\text{D}_2\text{O}$ -exchanged silica, however with a significantly lower percentage; this indicates the presence of hydrogen-bonded silanols in the  $\text{D}_2\text{O}$ -exchanged M-5 Cab-O-Sil. We suggest that these hydrogen-bonded silanols are interparticle silanols that are not accessible by  $\text{D}_2\text{O}$  molecule, but their arrangement is favorable for hydrogen bonding between each other.

After correcting for relaxation behavior in terms of the measured relaxation parameters ( $T_{1\rho}^{\text{H}}$ ,  $T_{\text{SiH}}$ , and  $T_1^{\text{H}}$ ), the amount of proton-bearing silanols (geminal plus single) remaining in the  $\text{D}_2\text{O}$ -exchanged sample is determined to be 32% of the silanols in untreated Cab-O-Sil silica. In addition to the possibility of internal (trapped) silanols, this large fraction of inaccessible silanols most likely includes at least a portion of interparticle silanols that may be located at sterically inaccessible sites. Since the CP-detected population of *hydrogen-bonded* silanols has been decreased dramatically by  $\text{D}_2\text{O}$  exchange, most of the hydrogen-bonded silanols are apparently exchangeable by  $\text{D}_2\text{O}$  molecules. Therefore, a large portion of the inaccessible interparticle silanols must exist as *isolated* silanols prior to exchange. A previous study of fumed silica by McFarlan and Morrow,<sup>4</sup> based on infrared spectroscopy, indicated that the peak at  $3750\text{ cm}^{-1}$  in the IR spectra is attributed to truly isolated SiOH groups; and a low-wavenumber shoulder was attributed to pairs of isolated SiOH groups on adjacent silicon atoms which are sufficiently close to slightly perturb each other. As mentioned above, for a water-treated Cab-O-Sil sample, isolated silanols still remain, rather than hydrogen bonding to water molecules in the presence of excess water. This fact is consistent with the conclusion that they are not readily accessible to form hydrogen bonds with  $\text{H}_2\text{O}$  molecules.

**Additional  $^1\text{H}$ – $^{29}\text{Si}$  CP  $^{29}\text{Si}$  NMR Experiments.** Additional experiments based on  $^{29}\text{Si}$  CP-MAS techniques described previously<sup>66</sup> have been carried out to explore the characteristics of  $^{29}\text{Si}$  signals of silanols of Cab-O-Sil silica. One such technique is the  $^1\text{H}$ – $^{29}\text{Si}$  dipolar-dephasing (interrupted decoupling)  $^{29}\text{Si}$  CP-MAS experiment. In this experiment, after the initial CP contact period, a  $2\tau$  dipolar-dephasing period (with  $180^\circ$   $^1\text{H}$  and  $^{29}\text{Si}$  pulses in the middle) is inserted before data acquisition to allow  $^1\text{H}$ – $^{29}\text{Si}$  dipolar dephasing to occur. During the dephasing period, the isotropic part of the  $^{29}\text{Si}$  chemical shift can refocus for any interrupt time  $2\tau$ , whereas the anisotropic part of the  $^{29}\text{Si}$  chemical shift can refocus completely only when  $2\tau$  is equal to  $2n\tau_r$ , where  $n$  is an integer and  $\tau_r$  is the MAS rotation period. To the extent that the  $^1\text{H}$ – $^{29}\text{Si}$  dipolar interaction is inhomogeneous, it will refocus completely only for any  $2\tau$  value equal to  $n\tau_r$ . A homogeneous  $^1\text{H}$ – $^{29}\text{Si}$  dipolar interaction cannot refocus completely for any choice of  $\tau$ .

(85) Parfitt, G. D.; Sing, K. S. W. *Characterization of Powder Surfaces*; Academic Press: London, New York, San Francisco, 1976; pp 353–420.

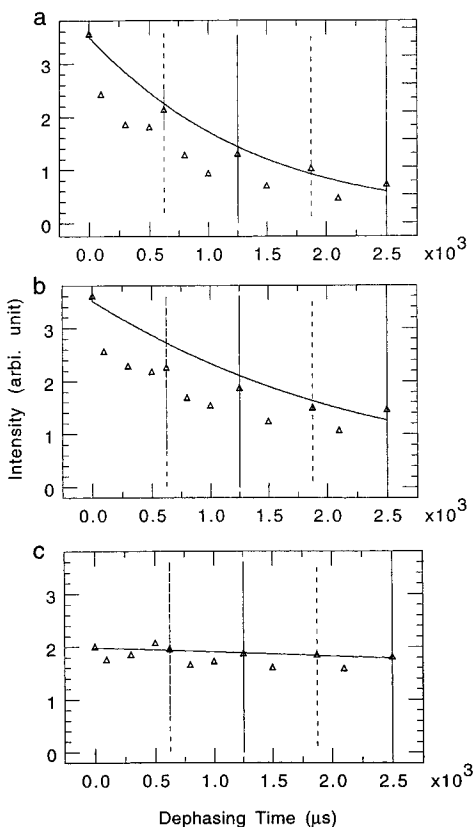


**Figure 14.** Plots of the deconvoluted peak intensities of the  $^{29}\text{Si}$  CP-MAS NMR spectra of untreated HS-5 Cab-O-Sil *vs*  $^1\text{H}$ - $^{29}\text{Si}$  dipolar-dephasing time, up to four rotor periods: (a) geminal silanols, (b) single silanols, and (c) siloxane silicons. CP contact time 5 ms; MAS speed 1.6 kHz. Vertical dashed lines show odd numbers of rotor periods and vertical solid lines show even numbers of rotor periods. The fitting curves represent the best fits, from which  $T_2'$  was derived.

Figure 14 shows, from this kind of experiment, plots of the deconvoluted peak intensities corresponding to the three types of silicon sites of the untreated M-5 Cab-O-Sil silica *vs* the dipolar-dephasing period (which ranged from 0 to more than  $4t_{\text{rot}}$ ). Focusing on the points at  $2\tau = 0$ ,  $2t_{\text{rot}}$ , and  $4t_{\text{rot}}$ , one sees that the peak intensity corresponding to geminal silanols ( $-89$  ppm) decays markedly with increasing  $^1\text{H}$ - $^{29}\text{Si}$  dipolar-dephasing time; the peak intensity corresponding to single silanols ( $-99$  ppm) decays less rapidly with increasing  $^1\text{H}$ - $^{29}\text{Si}$  dipolar dephasing time, while the peak intensity corresponding to  $\text{Q}_4$  ( $-109$  ppm) oscillates, but does not decay substantially.

A  $^1\text{H}$ - $^{29}\text{Si}$  dipolar interaction behaves homogeneously over a rotor period when (a) the  $^1\text{H}$  spin states change by chemical exchange or  $^1\text{H}$ - $^1\text{H}$  flip-flops generated by  $^1\text{H}$ - $^1\text{H}$  dipolar interactions, (b) the rate of molecular motion of the  $^1\text{H}$ - $^{29}\text{Si}$  internuclear vector is in the vicinity of the MAS speed, and/or (c) the  $^{29}\text{Si}$  spin states change by chemical exchange or  $^{29}\text{Si}$ - $^{29}\text{Si}$  flip-flops due to  $^{29}\text{Si}$ - $^{29}\text{Si}$  dipolar interactions. One expects that this third possibility can be neglected, due to the chemical nature of the system and the low natural abundance of  $^{29}\text{Si}$ . The total contribution  $(T_2)^{-1}$  of intrinsic  $^{29}\text{Si}$  transverse relaxation to the dipolar-dephasing constant  $(T_2')^{-1}$  was measured by a Hahn spin-echo experiment and found to be  $19^{-1}$ ,  $39^{-1}$ , and  $80^{-1} \text{ ms}^{-1}$ , respectively, for the geminal silanol, single silanol and  $\text{Q}_4$  peaks, respectively.

Because all of the inhomogeneous contributions (the CSA and the inhomogeneous part of the  $^1\text{H}$ - $^{29}\text{Si}$  dipolar interaction) refocus each time that  $2\tau$  equals an even number of rotor periods ( $2nt_r$ ), it becomes feasible to distinguish the homogeneous and

**Table 6.**  $T_2'$  values of M-5 Cab-O-Sil Obtained in  $^{29}\text{Si}$  CP-MAS Dipolar-Dephasing Experiments at Various MAS Speeds

MAS speed (kHz)	rotor period (ms)	$T_2'$ (ms)		
		$\text{Q}_2$	$\text{Q}_3$	$\text{Q}_4$
1.2	825	0.90	1.6	6.5
1.6	625	1.5	3.0	11
2.0	500	1.4	3.0	15

inhomogeneous  $^1\text{H}$  spin behaviors by monitoring the intensity of the  $^{29}\text{Si}$  CP-MAS signal as a function of the dipolar-dephasing time in terms of rotor periods. The loss of  $^{29}\text{Si}$  magnetization at even numbers of rotor periods, which can often be represented by a simple exponential function with a time constant  $T_2'$ , reflects the homogeneous character of  $^1\text{H}$ - $^{29}\text{Si}$  dipolar interactions, which may also reflect the homogeneous character of  $^1\text{H}$ - $^1\text{H}$  dipolar interactions. Figure 14 shows the best-fit exponential decay for the data points corresponding to  $2\tau = 2nt_r$ . The time constants,  $T_2'$ , obtained from these plots for each of the three silicon sites of untreated M-5 Cab-O-Sil silica, measured at three different spinning speeds, are summarized in Table 6.

Inspection of Table 6 shows qualitatively that higher spinning rates correspond to larger  $T_2'$  values. Presumably higher-speed MAS suppresses  $^1\text{H}$ - $^1\text{H}$  spin diffusion by partially averaging  $^1\text{H}$ - $^1\text{H}$  dipolar interactions,<sup>86-90</sup> rendering the  $^1\text{H}$ - $^{29}\text{Si}$  dipolar interactions less homogeneous and yielding larger  $T_2'$  values. If the  $T_2'$  decay were due entirely to chemical exchange or molecular motion,  $T_2'$  should be independent of the magic-angle spinning speed, unless the time constants characteristic of these processes were on the order of  $t_r$ . Molecular motion or chemical exchange at this rate (1–2 kHz) could broaden the peaks substantially, if the excursions of resonance frequencies were large enough to contribute substantially to  $(T_2')^{-1}$ , so it appears that  $^1\text{H}$ - $^1\text{H}$  spin diffusion must take place among the various hydroxyl groups on the Cab-O-Sil silica surface.

Additional dramatic evidence of  $^1\text{H}$ - $^1\text{H}$  spin exchange in Cab-O-Sil silicas is seen in the  $^{29}\text{Si}$  CP-MAS spectra obtained with the  $^1\text{H}$  decoupler turned off during detection. MAS should still average the  $^1\text{H}$ - $^{29}\text{Si}$  dipolar interaction during detection, yielding a corresponding spinning sideband pattern, to the extent that this interaction behaves inhomogeneously, i.e., to the extent that the  $^1\text{H}$ - $^{29}\text{Si}$  dipolar interaction is not altered (by chemical reaction, motion, or  $^1\text{H}$ - $^1\text{H}$  flip-flops) during a MAS rotation period.<sup>66</sup> Figure 15 shows proton-decoupled  $^{29}\text{Si}$  CP-MAS NMR spectra (top), along with the corresponding proton-coupled spectra (bottom), obtained on untreated M-5 Cab-O-Sil silica at three different MAS speeds. From the computer simulated/deconvoluted spectra (also shown in Figure 15), the results from which are summarized in Table 7, it can be seen that at each of the three MAS speeds, the line widths of the peaks for geminal and single silanols in the proton-coupled spectra are much larger than those of the corresponding proton-decoupled spectra. However, the line width of the siloxane peak is hardly changed when proton decoupling is turned off. The broadening effect on the silanol peaks in the proton-coupled spectra of Cab-O-Sil seen in Figure 15 must be due to the homogeneous character of  $^1\text{H}$ - $^{29}\text{Si}$  dipolar interaction, which in turn is due to changes in the  $^1\text{H}$ - $^{29}\text{Si}$  dipolar interaction during a rotor period because of  $^1\text{H}$ - $^1\text{H}$  flip-flops, chemical exchange, and/or molecular

(86) Kessemeyer, H.; Norberg, R. E. *Phys. Rev.* **1967**, *155*, 321.

(87) Haerberlen, U.; Waugh, J. S. *Phys. Rev.* **1969**, *185*, 420.

(88) Kubo, A.; McDowell, C. A. *J. Chem. Soc., Faraday Trans. 1* **1988**, *84*, 3713.

(89) Brunner, E.; Fenzke, D.; Freude, D.; Pfeifer, H. *Chem. Phys. Lett.* **1990**, *169*, 591.

(90) Brunner, E.; Freude, D.; Gerstein, B. C.; Pfeifer, H. *J. Magn. Reson.* **1990**, *90*, 90.

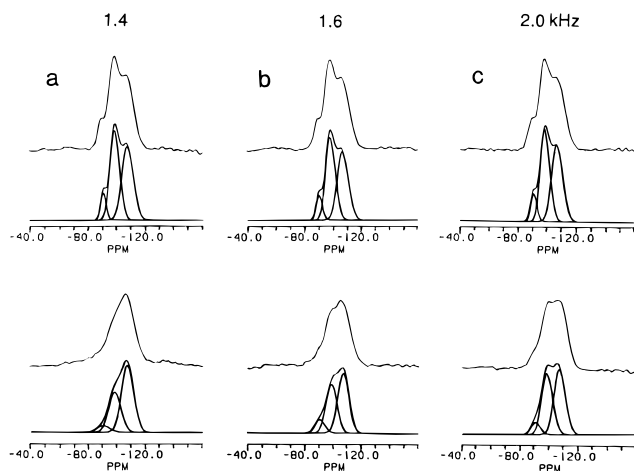


**Figure 15.** Proton-decoupled (top spectrum of each set) and proton-coupled (bottom spectrum of each set)  $^{29}\text{Si}$  CP-MAS spectra of untreated HS-5 Cab-O-Sil at three different MAS speeds, as indicated: (a) 1.4 kHz, 60 000 accumulations, (b) 1.6 kHz, 40 600 accumulations, and (c) 2.0 kHz, 40 000 accumulations. Computer simulated spectrum and individual deconvoluted contributions are shown below each corresponding experimental spectrum. CP contact time 5 ms.

**Table 7.** Line Widths and Peak Areas Derived for Deconvoluted Peaks of  $^{29}\text{Si}$  CP-MAS Spectra Obtained with and without  $^1\text{H}$  Decoupling

MAS speed	$^1\text{H}$ decouple	peak	LW <sub>HM</sub> ( $\times 10$ Hz) <sup>a</sup>	peak area <sup>b</sup>
1.4 kHz	yes	Q <sub>2</sub>	22	16
	yes	Q <sub>3</sub>	38	95
	yes	Q <sub>4</sub>	45	92
	no	Q <sub>2</sub>	52	10
	no	Q <sub>3</sub>	48	58
	no	Q <sub>4</sub>	47	94
1.6 kHz	yes	Q <sub>2</sub>	24	13
	yes	Q <sub>3</sub>	38	70
	yes	Q <sub>4</sub>	45	68
	no	Q <sub>2</sub>	40	12
	no	Q <sub>3</sub>	44	48
	no	Q <sub>4</sub>	45	61
2.0 kHz	yes	Q <sub>2</sub>	25	12
	yes	Q <sub>3</sub>	38	65
	yes	Q <sub>4</sub>	45	63
	no	Q <sub>2</sub>	35	8.8
	no	Q <sub>3</sub>	43	54
	no	Q <sub>4</sub>	45	60

<sup>a</sup> Line width at half maximum. <sup>b</sup> Arbitrary units. Estimated error:  $\pm 5\%$  (of the number given).

motion. The extent of the resulting broadening reflects the combined effect of these changes and the strength of the  $^1\text{H}$ – $^{29}\text{Si}$  dipolar interactions.

The geminal silanol peak at about  $-89$  ppm in the proton-coupled  $^{29}\text{Si}$  NMR spectra shown in Figure 15 is so severely broadened that this region is hardly recognizable as a peak, especially at lower MAS speeds. This broadening effect is harsher than in the single silanol peak, indicating that the spin diffusion rate is faster among the geminal silanol protons than that in the single silanol protons.

Inspection of Table 7 reveals that at all three MAS speeds examined, the single-silanol peak seems to lose roughly one-third of its fully decoupled peak area in the spectra of Figure 15 obtained without proton decoupling. This apparent loss of intensity can be attributed to the silanols that experience very strong  $^1\text{H}$ – $^{29}\text{Si}$  dipolar interactions; the  $^{29}\text{Si}$  signals of these silanols are broadened and apparently "lost" to the extent that the "lost" intensity cannot be resolved from baseline noise without the line-narrowing provided by high-power  $^1\text{H}$  decou-

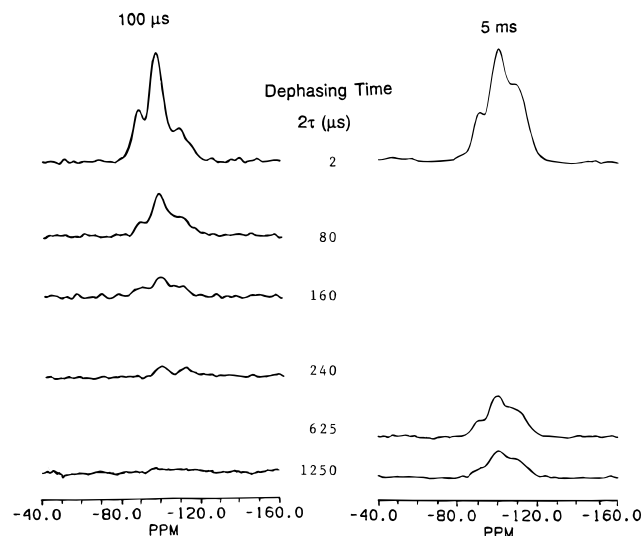


**Figure 16.**  $^{29}\text{Si}$  CP-MAS NMR spectra of untreated HS-5 Cab-O-Sil obtained as a function of  $^1\text{H}$ – $^1\text{H}$  dipolar-dephasing periods ( $2\tau$ ) prior to  $^1\text{H}$ – $^{29}\text{Si}$  cross polarization; (left side) CP contact time  $100\ \mu\text{s}$ , repetition delay  $0.6\ \text{s}$ , each spectrum is the result of 20 000 accumulations; (right side) CP contact time  $5\ \text{ms}$ , repetition delay  $0.6\ \text{s}$ , each spectrum is the result of 10 000 accumulations. One rotor period,  $625\ \mu\text{s}$ ; two rotor periods,  $1.25\ \text{ms}$ .

pling. The redistribution of intensity to spinning sidebands is not detectable in the spectra available.

Qualitatively, the behavior displayed in Figure 15 is consistent with the discussion of the  $^1\text{H}$ – $^{29}\text{Si}$  dipolar-dephasing experiment discussed above. Both types of experiments show the involvement of  $^1\text{H}$  spin diffusion in the  $^{29}\text{Si}$  NMR behavior of geminal silanols and single silanols, especially the former, on the Cab-O-Sil silica surface, reflecting the  $^1\text{H}$ – $^1\text{H}$  proximity associated with hydrogen bonding.

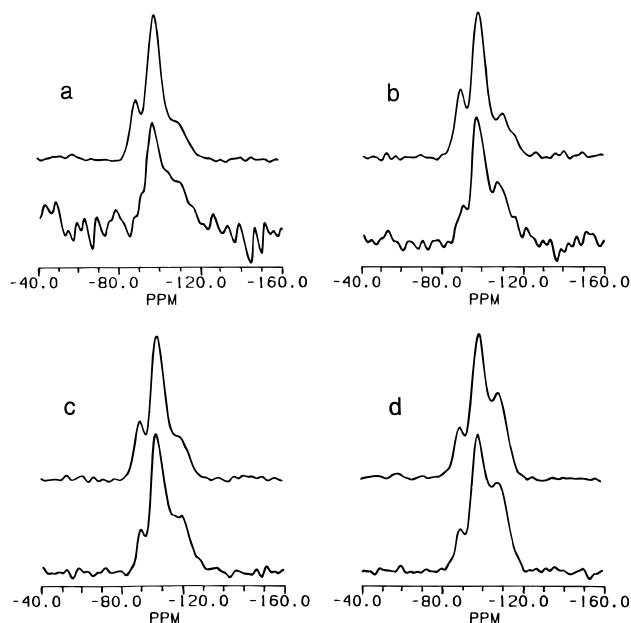
A very direct correlation of  $^1\text{H}$  CRAMPS dipolar-dephasing behavior, as represented in Figure 7, with  $^{29}\text{Si}$  CP-MAS signals is obtained in a  $^{29}\text{Si}$ -monitored  $^1\text{H}$ – $^1\text{H}$  dipolar-dephasing experiment, in which  $^1\text{H}$ – $^{29}\text{Si}$  cross polarization is used to transfer information on  $^1\text{H}$ – $^1\text{H}$  dipolar dephasing to  $^{29}\text{Si}$  spin sets for observation. In this experiment,<sup>66</sup> after an initial  $90^\circ$   $^1\text{H}$  pulse and prior to  $^1\text{H}$ – $^{29}\text{Si}$  cross polarization, there is a  $^1\text{H}$ – $^1\text{H}$  dipolar-dephasing period ( $2\tau$ , with a  $180^\circ$   $^1\text{H}$  pulse in the middle) with  $^{29}\text{Si}$  decoupling, during which changes in  $^1\text{H}$  spin states and dipolar interactions (due to  $^1\text{H}$ – $^1\text{H}$  flip-flops, chemical exchange, and/or molecular motion) cause a nonrefocusable decay of transverse  $^1\text{H}$  magnetization. As discussed above for the  $^1\text{H}$ – $^{29}\text{Si}$  dipolar dephasing experiment, the inhomogeneous behavior is refocused when  $2\tau = n\tau_r$ . Hence, magnetization of those protons involved in the strongest (shortest, least mobile) hydrogen bonds is most effectively dephased during  $2\tau = 2n\tau_r$  and unavailable for CP transfer to  $^{29}\text{Si}$ .

Figure 16 shows  $^{29}\text{Si}$  CP-MAS NMR spectra obtained via the  $^1\text{H}$ – $^1\text{H}$  dephasing  $^1\text{H}$ – $^{29}\text{Si}$  CP-MAS experiment, with various  $^1\text{H}$ – $^1\text{H}$  dipolar dephasing periods ( $2\tau$ ), including  $625\ \mu\text{s}$  (one rotor period) and  $1250\ \mu\text{s}$  (two rotor periods), and CP contact times of  $100\ \mu\text{s}$  (left side) and  $5\ \text{ms}$  (right side). At one rotor period of dipolar dephasing, the intensity of each peak in the  $^{29}\text{Si}$  CP-MAS spectrum has been dramatically attenuated, compared with the spectrum obtained with  $2\text{-}\mu\text{s}$  dipolar dephasing (which is essentially the same as a normal CP-MAS spectrum without any dipolar-dephasing period). The overall attenuation of the transverse  $^1\text{H}$  magnetization with  $2\tau = n\tau_r$  for odd  $n$  results from the anisotropic part of the  $^1\text{H}$  chemical shift and from homogeneous character in the  $^1\text{H}$ – $^1\text{H}$  dipolar interaction, combined with changes in the  $^1\text{H}$  spin states through

$^1\text{H}$ – $^1\text{H}$  flip-flops or chemical exchange and changes in the  $^1\text{H}$ – $^1\text{H}$  dipolar interaction due to molecular motion. Both the isotropic part of the  $^1\text{H}$  chemical shift and the inhomogeneous portion of a  $^1\text{H}$ – $^1\text{H}$  dipolar interaction refocus at  $2\tau = n\tau_r$  and should therefore not contribute to the attenuation of the  $^{29}\text{Si}$  CP-MAS peak intensities of the spectra on the right side of Figure 16 (e.g., for  $2\tau = \tau_r = 625 \mu\text{s}$ ). When the  $^1\text{H}$ – $^1\text{H}$  dipolar dephasing time,  $2\tau$ , increases from  $\tau_r$  to  $2\tau_r$ , the peak intensities in the spectrum shown in Figure 16 decrease (by  $\sim 35\%$ ), but not as much as when changing  $2\tau$  from  $2 \mu\text{s}$  to  $625 \mu\text{s}$  (about 63%). All three of the spectra on the right side of Figure 16 (5 ms contact time) have nearly the same line shape and relative peak intensities, with perhaps a somewhat attenuated and broadened  $\text{Q}_2$  peak and a somewhat broadened  $\text{Q}_4$  peak, essentially differing from each other mainly in total spectral intensity. Hence, because of averaging that occurs among protons via spin exchange in a 5-ms period, all three types of silicons appear to be affected nearly equally by  $^1\text{H}$ – $^1\text{H}$  dipolar dephasing.

During  $^1\text{H}$ – $^{29}\text{Si}$  cross polarization in the experiment represented in Figure 16,  $^1\text{H}$ – $^1\text{H}$  spin–spin flip-flops and chemical exchange still operate and tend to bring the interacting protons toward a mutual equilibration. Therefore, if one wishes to utilize the CP-generated  $^{29}\text{Si}$  NMR signal to monitor the status of  $^1\text{H}$  spin sets, then the cross polarization contact time should be kept as short as possible to reflect the specific  $^1\text{H}$ – $^1\text{H}$  dipolar dephasing behavior of individual  $^1\text{H}$  spin sets. Although a very large ( $2.5\text{-cm}^3$ ) MAS rotor was employed in these experiments, an acceptable signal-to-noise ratio could be achieved only with a CP contact time of at least  $100 \mu\text{s}$ . The left side of Figure 16 shows the  $^{29}\text{Si}$  CP-MAS NMR spectra obtained on untreated HS-5 with a  $100\text{-}\mu\text{s}$  CP contact time. The  $^1\text{H}$  CRAMPS results on untreated HS-5 Cab-O-Sil discussed above indicated that an  $80\text{-}\mu\text{s}$   $^1\text{H}$ – $^1\text{H}$  dipolar-dephasing time was long enough to largely eliminate  $^1\text{H}$  magnetization due to the strongly coupled  $^1\text{H}$  spin reservoir generated by the hydrogen-bonded silanols. However, Figure 16 indicates that, with a  $80\text{-}\mu\text{s}$   $^1\text{H}$ – $^1\text{H}$  dipolar dephasing time prior to  $^1\text{H}$ – $^{29}\text{Si}$  cross polarization with a  $100\text{-}\mu\text{s}$  CP contact time, the peak intensities of *both* silanols and siloxanes are attenuated (about 62%), but not dephased completely. This residual signal after a  $80\text{-}\mu\text{s}$  dipolar-dephasing period is due to the existence of isolated silanols of both single and geminal silanol types, for which, as shown in the  $^1\text{H}$  CRAMPS experiments, the  $^1\text{H}$  magnetization dephases with a much slower rate. With a  $240\text{-}\mu\text{s}$   $^1\text{H}$ – $^1\text{H}$  dipolar-dephasing period prior to a  $100\text{-}\mu\text{s}$   $^1\text{H}$ – $^{29}\text{Si}$  CP contact time,  $^1\text{H}$  spin polarization responsible for the geminal silanol  $^{29}\text{Si}$  signal, and to a lesser extent that responsible for single silanols, are largely depleted relative to the  $^1\text{H}$  magnetization responsible for  $^1\text{H}$ – $^{29}\text{Si}$  CP for  $\text{Q}_4$  silicons. The faster dephasing rate seen for geminal silanol protons than that in single silanols indicates that a larger proportion of geminal silanol protons is involved with hydrogen bonding, in which  $^1\text{H}$ – $^1\text{H}$  dipolar interactions are stronger. As the individual  $^1\text{H}$ – $^1\text{H}$  dipolar dephasing behaviors of the three different  $^1\text{H}$  spin sets were reflected by the CP-generated  $^{29}\text{Si}$  signals in the spectra on the left side of Figure 16, we can conclude that the  $100\text{-}\mu\text{s}$  cross polarization contact time is short enough to avoid completely “undermining” the “selective” cross polarization strategy by rotating-frame  $^1\text{H}$  spin exchange.

Inspection of spectra on the left side of Figure 16 reveals that most of the  $^1\text{H}$  spin polarization responsible for  $^1\text{H}$ – $^{29}\text{Si}$  CP is destroyed by a  $^1\text{H}$ – $^1\text{H}$  dipolar dephasing time of  $240 \mu\text{s}$  prior to a  $100\text{-}\mu\text{s}$   $^1\text{H}$ – $^{29}\text{Si}$  cross polarization, and this effect is especially harsh for geminal silanols. If the siloxane  $^{29}\text{Si}$  CP-MAS peak derived its  $^{29}\text{Si}$  magnetization completely by cross



**Figure 17.**  $^{29}\text{Si}$  CP-MAS NMR spectra of untreated HS-5 Cab-O-Sil with  $2 \mu\text{s}$  (top spectrum of each set) and two rotor periods (1.25 ms, bottom spectrum of each set) of  $^1\text{H}$ – $^1\text{H}$  dipolar dephasing prior to four different  $^1\text{H}$ – $^{29}\text{Si}$  cross polarization contact times,  $t_{\text{CP}}$ . Repetition delay: (a)  $t_{\text{CP}} = 100 \mu\text{s}$  (top spectrum, 20 000 accumulations; bottom spectrum, 25612 accumulations); (b)  $t_{\text{CP}} = 300 \mu\text{s}$  (top spectrum, 22 600 accumulations; bottom spectrum, 40 000 accumulations); (c)  $t_{\text{CP}} = 1 \text{ ms}$  (top spectrum, 1000 accumulations; bottom spectrum, 34 000 accumulations); (d)  $t_{\text{CP}} = 5 \text{ ms}$  (top spectrum, 1000 accumulations; bottom spectrum, 10 000 accumulations).

polarization from only the silanol protons, then the siloxane  $^{29}\text{Si}$  signal would be depleted (by the  $^1\text{H}$ – $^1\text{H}$  dipolar-dephasing process) by the same attenuation factor as that of the silanol  $^{29}\text{Si}$  peaks. Hence, we conclude that cross polarization from some other source contributes at least some intensity to the siloxane peak in  $^{29}\text{Si}$  CP-MAS spectra obtained with  $^1\text{H}$ – $^1\text{H}$  dipolar-dephasing times  $\geq 240 \mu\text{s}$ . This non-silanol proton source for cross polarization might be physisorbed water or water that is “trapped” in the interior of the silica structure; in the Cab-O-Sil case, water could perhaps be easily trapped by rapid cooling during synthesis. “Trapped” water protons are much more likely than surface-physisorbed water as the non-silanol proton source, because the protons of the “trapped” water might be much closer to siloxane silicons that constitute the interior structure of Cab-O-Sil than the exterior silanol protons are to their neighboring  $\text{Q}_4$  silicons.

Figure 17 shows  $^1\text{H}$ – $^1\text{H}$  dephased  $^{29}\text{Si}$  CP-MAS spectra obtained on an untreated HS-5 Cab-O-Sil sample, based on a  $^1\text{H}$ – $^1\text{H}$  dephasing period  $2\tau = 2\tau_r$  (1.25 ms) prior to cross polarization, using CP contact times of 0.1, 0.3, 1, and 5 ms. All spectra in this figure are scaled to equal heights of the single silanol ( $-99 \text{ ppm}$ ) peak to facilitate relative intensity comparisons. With a 0.1-ms contact time, the *relative* intensity of the  $^{29}\text{Si}$  NMR signal corresponding to geminal silanols is almost eliminated completely, whereas the *relative* intensity of the siloxane peak is enhanced. With a longer CP contact time of 0.3 ms, the same effects are seen in the spectra, but less dramatically. During the 0.3-ms cross polarization period, spin exchange permits the  $^1\text{H}$  spin reservoir of the geminal silanols to recover somewhat, as indicated by a substantial *relative* intensity of the  $-89\text{-ppm}$  peak.

While direct long-range cross polarization of the geminal silanol silicons from single-silanol proton magnetization that survives dephasing is *a priori* a possible explanation of the

behavior seen in Figure 17,  $^1\text{H}$  spin exchange among the silanols is a more likely (i.e., more efficient) mechanism. The results presented in Figure 17 show that the  $^1\text{H}$ – $^1\text{H}$  rotating-frame spin diffusion time constant is on the order of hundreds of microseconds, while cross polarization time constants for silanol protons to their nearest silicons are on the order of a few milliseconds. Cross polarization time constants for silicons at larger distances would be even larger. Hence,  $^1\text{H}$  spin exchange is the more likely mechanism for determining the  $^{29}\text{Si}$  intensities of geminal and single silanols during the 0.3-ms CP contact period represented in Figure 17b. The communication among different silanol  $^1\text{H}$  spin reservoirs in Cab-O-Sil is sufficiently fast that in a short 0.3-ms CP contact time period some geminal silanol proton magnetization is re-established, even with a 1.25-ms  $^1\text{H}$ – $^1\text{H}$  dipolar dephasing time, which is essentially long enough to eliminate the proton magnetization of geminal silanols. More recovery of  $^1\text{H}$  magnetization in the geminal silanol reservoir is found with 1- and 5-ms CP contact periods. The three peaks in the  $^{29}\text{Si}$  CP-MAS spectra in Figures 17c and 17d achieve relative intensities that are close to their values in the absence of a prior  $^1\text{H}$ – $^1\text{H}$  dipolar dephasing period.

From deconvolutions (not shown here)<sup>73</sup> of the spectra presented in Figure 17, one can determine the sum of integrated intensities of the peaks corresponding to single silanols and geminal silanols in Figures 17a and 17b and use them to determine a silanol intensity ratio between the spectra obtained with 2  $\mu\text{s}$  and two rotor periods of dipolar dephasing. When the intensities used in computing this ratio are normalized to the same number of accumulations, this ratio is determined to be about 5:1 for each of these two CP contact times. That is, approximately 4/5 of the combined signal intensities of these two types of silanol  $^{29}\text{Si}$  signals is destroyed by a 1.25-ms duration of  $^1\text{H}$ – $^1\text{H}$  dipolar dephasing prior to  $^1\text{H}$ – $^{29}\text{Si}$  CP. However, this magnitude of signal reduction is clearly not the case for the siloxane peak in the same spectra, which has a corresponding ratio of 3:1 for the spectra obtained with 2  $\mu\text{s}$  and two rotor periods of dipolar dephasing. These results would seem to indicate that the silanol silicons and siloxane silicons have different CP  $^1\text{H}$  sources for either a 0.1- or a 0.3-ms CP contact time.

“Trapped” water molecules have already been implicated as non-silanol proton CP sources for siloxane cross polarization to explain the results shown in spectra on the left side of Figure 16 for a CP contact time of 0.1 ms. If the non-silanol portion of the  $^1\text{H}$  spin reservoir responsible for siloxane cross polarization were in communication with the  $^1\text{H}$  spin reservoir responsible for silanol cross polarization, the siloxane  $^1\text{H}$  spin reservoir would perturb the silanol protons as they achieved this pseudo-equilibrium. Actually, with 1 to 5 ms CP contact time (Figures 17c and 17d), the 2  $\mu\text{s}$ :6.25 ms intensity ratio for both silanols and siloxanes is 3:1, implying that spin exchange between the  $^1\text{H}$  spin reservoirs of silanol groups and physisorbed water is slow relative to a time scale of 1 ms, but occurs within 1 to 5 ms. These results imply structurally that physisorbed water molecules and various silanols are not far from each other, say  $\leq 6$  Å.

The most accepted view of the structure of fumed silicas is that of small secondary particles attached together to form chains with a “coordination number” of about 3, given no microporosity.<sup>91</sup> The secondary particles are formed by closed-packed, nonporous, small (about 1.5 nm in diameter) primary particles.<sup>85</sup> Even with primary particles of such small size, interparticle microporosity might be detected by nitrogen adsorption if the

coordination number of the primary particle were 6 (cubic packing), so investigators have been inclined toward the view that packing within the secondary structure is probably characterized by a high coordination number. The small particle size and the high coordination number render the interparticle region a significant contribution to the total surface area.

The interparticle contact area is referred to as the area in which silanols on the two adjacent silica particles can interact with each other. When silanols on two adjacent particles are hydrogen bonded to each other, the maximum Si-to-Si distance between the two particles would be the sum of the maximum hydrogen bonding O---O distance (say, 3.3 Å), plus  $2 \times 1.63$  Å (Si–O distance<sup>92</sup>), which is about 6.6 Å. Water molecules can easily go into this contact area, because the effective diameter of a water molecule is only about 2.8 Å.<sup>93</sup> Therefore, not all interparticle contact areas are inaccessible to water molecules. For a simple model of interparticle contact, we assume that the area that is inaccessible to water molecules by virtue of contact between two 1.5-nm-diameter spherical silica particles is the area of a spherical cap in which the depth of the cap is half the “diameter” of a “spherical” water molecule (0.14 nm). For this model we estimate, on the basis of simple analytic geometry, that the fraction of spherical surface area that is inaccessible to water molecules is 0.05 (5%) per contact. For a coordination number of 6–12, the inaccessible area comes to 30 to 50% of the total surface area of a fumed silica, which is a very substantial fraction. This estimated range of values is, of course, dependent on the particle size, the coordination number, and the assumption regarding the detailed meaning of a term like “interparticle contact areas—inaccessible to water molecules”, and could vary over a large range. In any case, this range of values is consistent with the value 32% that was found for the percentage of silanol protons of Cab-O-Sil that are not  $\text{D}_2\text{O}$  exchangeable (*vide supra*). For 20-nm-diameter particles, the value per contact is reduced to 0.6% from 5%. Hence we can expect that the contact area between silica gel particles (usually with diameters larger than 50 nm) can be neglected without any doubt. In other words, almost all the surface silanols in silica gel should be accessible by water molecules and therefore can form hydrogen bonds to water molecules in untreated samples. This is a major difference between silica gel and fumed silica.

$^1\text{H}$  CRAMPS and high-speed MAS-only experiments indicate that *isolated* silanols constitute about 15% of the total silanols on an untreated Cab-O-Sil silica surface (Table 2). Silicas consisting of 20-nm (diameter) particles would not have this much (15%) inaccessible interparticle area. We therefore concur with the view that the primary particles of fumed silica are extremely small, possibly with a 1.0–1.5-nm diameter. In addition to the 30–50% inaccessible (not hydrogen bonded to water) silanols that one might expect from a very simple model of interparticle contacts of silica particles of 1.0–1.5-nm diameter, one would also expect additional numbers of silanols (an additional fraction of the fumed silica particle surface) to be inaccessible to  $\text{D}_2\text{O}$  exchange or hydrogen bonding with water due to interstitial “voids” that occur in the close packing of particles. Thus, if the fumed silica particles really are as small as 1.0–1.5 nm, and really are close packed, then a substantial fraction of the interparticle contact areas in the outer layers of particle clusters must be capable of interacting (hydrogen bonding) with water. Indeed, perhaps it is the properties of the secondary particles that are responsible for some of the patterns observed in this study.

(91) Broekhoff, J. C. P.; Linsen, B. G. *Physical and Chemical Aspects of Adsorbents and Catalysts*; Academic Press: London and New York.

(92) Wells, F. A. *Structural Inorganic Chemistry* 5th ed.; Clarendon Press: Oxford, UK, 1984; p 1000.

(93) Reference 92, p 656.



**Summary and Conclusions.** Perhaps the most interesting feature of the Cab-O-Sil surface is the existence in the untreated sample of *both* isolated and hydrogen-bonded silanols, in contrast to the untreated silica gel surface, on which all silanols are hydrogen bonded to each other and/or adsorbed water molecules. Both single silanols and geminal silanols in untreated or water-saturated Cab-O-Sil silica can exist as hydrogen bonded or non-hydrogen bonded, i.e., isolated, but the isolated silanol site is present on the silica gel surface only after evacuation. Cab-O-Sil silica is produced at high temperatures in a flame, and therefore it is reasonable to assume that some surface hydroxyl groups are trapped at the contact points between two or more silica globules obtained during the process of aggregation. Some of these "interparticle" hydroxyl groups, as well as silanols in interstices between particles, apparently have little chance to be accessible by water molecules because of steric hindrance.

Cab-O-Sil silica is non-porous and physisorbed molecules held only on the exterior surface. This is consistent with the  $^1\text{H}$  NMR results that demonstrate the facile adsorption and desorption of moisture (*vide supra*). Weakly-bounded physisorbed water on the Cab-O-Sil surface can be depleted by spinning the sample, if the sample tube is not sealed. This behavior is typically not found for the silica gel system, probably because the adsorbed water is entrapped in pores in the case of silica gel.

Dehydration studies of the Cab-O-Sil system reveal that the elimination of water adsorbed in the molecular form is basically complete at 25 °C under vacuum ( $3 \times 10^{-3}$  Torr). The partial elimination of Cab-O-Sil's silanol coating occurs at about 225–350 °C. At higher temperatures, essentially only isolated silanols are left on the Cab-O-Sil surface.

Compared with silica gel,  $^{29}\text{Si}$  NMR spectra of Cab-O-Sil have larger line widths for all three types of silicon sites. This implies a larger dispersion of local surface geometries, e.g., wider range of variation of Si–O–Si angles between adjacent siloxane tetrahedra. Because of the high temperature (1700 °C) used in the production of Cab-O-Sil, more siloxane bridges with a variety of Si–O–Si bond angles can be locked in upon rapid cooling.

**Acknowledgment.** The authors acknowledge helpful discussions with Dr. I-Ssuer Chuang and partial support of this study by the National Science Foundation Grant No. CHE-9021003 and Grant No. F49620-95-1 from the Air Force Office of Scientific Research.

**Supporting Information Available:**  $^1\text{H}$  CRAMPS and  $^1\text{H}$  MAS-only spectra of HS-5 Cab-O-Sil (2 pages). Ordering information is given on any current masthead page.

JA954120W